

Recovery With Incomplete Knowledge: Fundamental Bounds on Real-Time Quantum Memories

Arshag Danageozian*

Hearne Institute for Theoretical Physics, Department of Physics and Astronomy,
and Center for Computation and Technology, Louisiana State University, Baton Rouge, Louisiana 70803, USA

The recovery of fragile quantum states from decoherence is the basis of building a quantum memory, with applications ranging from quantum communications to quantum computing. Many recovery techniques, such as quantum error correction (QEC), rely on the *a priori* knowledge of the environment noise parameter to achieve their best performance. However, such parameters are likely to drift in time in the context of implementing long-time quantum memories. This necessitates the use of a “spectator” system, which makes an estimate of the noise parameter in real time, then feeds the outcome back to the recovery protocol as a classical side-information. The memory qubits and the spectator system hence comprise the building blocks for a real-time (i.e. drift-adapting) quantum memory. In this article, I present information-theoretic bounds on the performance of such a spectator-based recovery. Using generalized distinguishability measures as a starting point, I show that there is a fundamental bound in the performance of any recovery operation, as a function of the entanglement fidelity of the overall dynamics. The lower bound for the diamond distance has a simple form, and a potentially broader range of applicability in quantum information. I provide information-theoretic characterizations of the incomplete knowledge of the noise parameter to the lower bound, using both diamond distance and quantum Fisher information. Finally, I provide fundamental bounds for multi-cycle recovery in the form of recurrence inequalities. The latter suggests that incomplete knowledge could be an advantage, as errors from various cycles can cohere. These results are illustrated for the approximate [4,1] code of the amplitude-damping channel and relations to various fields are discussed.

CONTENTS

I. Introduction	2	VI. Recovery Bounds in The Multi-Cycle Scenario	14
II. Preliminaries	3	A. The Multi-Cycle Case	14
A. Quantum States and Channels	3	B. Recurrence Inequalities for Composite	14
B. Quantum Fidelities	3	Average Channel Fidelity	14
C. Channel Twirlings	4	C. Contribution of The Spectator System	15
D. Generalized Distinguishability and Distance	4	D. Application to [4,1] Code of The	15
Measures	4	Amplitude-Damping Channel	15
III. Lower-Bounding Generalized Distinguishability	5	VII. Comparison With Previous Literature	16
Measures	5	A. Relation to Quantum Information-Theoretic	16
IV. Lower-Bounding Diamond Distance Using	7	Protocols	16
Entanglement Fidelity	7	B. Relation to Robustness of Channel-adapted	16
V. Fundamental Bounds on Recovery with	9	QEC	16
Incomplete Knowledge	9	C. Relation to [4,1] AD Code Literature	17
A. Information-Theoretic Bounds	9	D. Relation to Time-Dependent QEC	18
1. Fundamental Limitations for Perfect	9	VIII. Conclusion and Open Questions	18
Knowledge Scenario	9	IX. Acknowledgements	19
2. Contribution of the Spectator System	9	References	19
B. Spectator Dynamics	10	A. χ -Matrix Representation of Quantum	21
C. Application to The [4, 1] Code of The	11	Channels	21
Amplitude-Damping Channel	11	B. Unitary t -designs	23
1. The Amplitude-Damping Channel	11	C. Comment on The Chaining Property	23
2. The Approximate [4, 1] Code	11	D. Upper-Bounding Generalized Distance	23
3. Entanglement Fidelity	12	Measures for State Recovery	23
		1. Single-Cycle Case	24
		2. Multi-Cycle Case	24

* Corresponding Author: arshag.danageozian@gmail.com

I. INTRODUCTION

Various important developments in quantum technologies have been targeted towards building high-fidelity quantum memories, which attempt to preserve the state of a quantum system from decoherence and various other noises. Quantum error correction (QEC) [1–3] and dynamical decoupling [4, 5] are two prime examples of such quantum technologies. These techniques generally benefit from the *apriori* knowledge of the noise surrounding the system of interest. For example, channel-adaptation techniques in QEC [6] have been shown to outperform general QEC codes, as they are given additional knowledge of the environment noise [7, 8]. Such techniques rely on some physical model of the (noisy) implementation medium of the memory and computational qubits. The noise model is partially built upon physical assumptions (e.g. in the choice of the Hamiltonians) and partially upon phenomenology. Hence, the former gives a physically motivated family of quantum dynamics $\{\mathcal{N}_\theta\}_{\theta \in \Theta}$ for the quantum state of the memory qubits [9], and the latter determines the value of the noise parameter θ such that the dynamics \mathcal{N}_θ fits the observed data the best.

Although being very powerful, a shortcoming of this approach is that the environment noise parameter is generally time-varying [10]. Hence, real-time techniques to track the change (drift) of the noise are necessary, assuming we want to operate quantum memories for times larger than the characteristic times of the drift [11]. This is true for various important setups, such as quantum networks, adaptive quantum communication protocols, and quantum computing.

Indeed, efforts have been made towards designing “spectator” systems that aid in detecting and tracking such changes [12–17]. Being subject to the same environment, the goal of the spectator system is to output an estimate of the noise parameter in real-time, which is then used as a classical side-information in various recovery protocols. The physical requirements of such systems are two-fold: (1) proximity to the memory/computational qubits, such that the spacial dependence of the noise parameter can be neglected, and (2) exhibiting faster dynamics than the memory qubits. The latter is necessary if the feedback information is to be useful for recovery. We showcase the functionality of the spectator system within a quantum memory using Figs. 1 and 2. Note that, since the memory and spectator systems are generally different physical systems with different couplings to the same environment, their dynamics will generally be described by different quantum channels with the same noise parameter, i.e. \mathcal{N}_θ and \mathcal{M}_θ , respectively.

There exist systems that satisfy the physical properties of a spectator system. For example, nitrogen-vacancy (NV) centers in diamond provide both a spectator system and a memory qubit. Namely, the nuclear spin degree

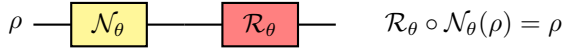


FIG. 1. Recovery with perfect knowledge (time flows from left to right). The recovery channel \mathcal{R}_θ is implemented using perfect knowledge of the noise parameter $\theta \in \Theta$ of the environment noise \mathcal{N}_θ .

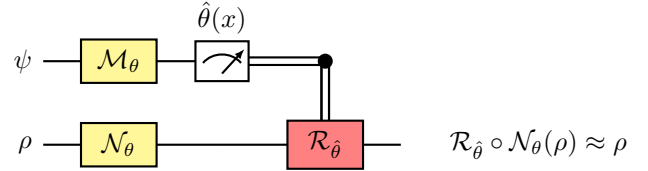


FIG. 2. Recovery with limited knowledge (time flows from left to right). The recovery channel $\mathcal{R}_{\hat{\theta}}$ is implemented based on the spectator’s best estimate $\hat{\theta}$ of the noise parameter $\theta \in \Theta$ of the environment noise \mathcal{N}_θ . The estimate is informed by the measurement outcome x of the spectator observable X , following the spectator dynamics \mathcal{M}_θ .

of freedom of its ^{14}N or ^{15}N atom comprises the memory qubit, whereas a nearly-closed three-level Λ system [18, 19], optically selected out of the electronic degrees of freedom of the NV center, comprises the spectator system [20, 21]. The fact that the characteristic times of the memory qubit ($\sim 100\mu\text{s}$) and the spectator system ($\sim 100\text{ns}$ [22]) differ by an order of 10^3 is what makes recovery techniques, such as QEC, valid for real-time quantum memories.

Although spectator systems are a promising building block for real-time (i.e. drift-adapting) quantum memories, we expect fundamental limitations to manifest nonetheless. This is based on the following physical intuition: In real time, the goal of the spectator system is to conduct a quantum estimation of the environment noise parameter θ . However, due to the quantum Cramer-Rao bound (QCRB) [23, 24], any unbaised estimate $\hat{\theta}$ of the noise parameter θ (in a finite time) will have a non-zero variance. Namely, $\text{Var}(\hat{\theta}) \geq 1/I_{\text{QF}}(\mathcal{M}_\theta)$, where $I_{\text{QF}}(\mathcal{M}_\theta)$ is the quantum Fisher information of the family of parametric channels $\{\mathcal{M}_\theta\}_{\theta \in \Theta}$ describing the spectator system dynamics (see Fig. 2). For a given setup, this fundamental uncertainty in the estimate $\hat{\theta}$ will manifest itself as a fundamental limitation of the specific recovery technique.

In this article, I formalize the above intuition by proving information-theoretic bounds on the performance of the spectator system in recovery protocols, considering QEC as an example. The results of the article are summarized below

1. Proof of a lower bound for generalized distinguishability measures between any two quantum channels (Theorem 1). I show that the lower bound

is a function of the entanglement fidelities of the individual channels, where the form of the function depends on the choice of the distinguishability measure used.

2. When the distinguishability measure is the diamond distance, the lower bound can be computed analytically and is equal to the difference between the entanglement fidelities of the two channels (Lemma 3 and Corollary 1). This generalizes a previous observation in [25] for the diamond distance between the identity channel and a depolarizing channel for qudits, as well as the analytic formula in [26] for the diamond distance between two depolarizing channels for qubits.
3. Information-theoretic characterization of the contribution of spectator systems in limited-knowledge recovery protocols. This characterization has two forms: (1) the diamond distance between the optimal and best-guess recovery operations for the given quantum noise (Theorem 2), and (2) the quantum Fisher information of the spectator dynamics (Theorem 3). This is illustrated for the [4,1] code of the amplitude-damping channel. I show that improvements upon the well-known approximate code [7] that are achieved by channel adaptation techniques [6, 8] (which is noise parameter dependent) are partially preserved, even in the incomplete knowledge scenario (Figs. 4 and 6).
4. Reformulation of an upper bound for the entanglement fidelity of multi-cycle recovery protocols (building upon a theorem of [27]) in the form of recurrence inequalities (Theorem 4). These bounds are growing in relevance, as multiple QEC rounds have been demonstrated in practice [28]. I show that a better recovery performance might be possible using spectator systems, as errors from different cycle numbers can cohere [27] (an effect that is exclusive to multi-cycle protocols), including errors from incomplete knowledge of the noise parameter. Finally, I illustrate the regions of better performance for the [4,1] code of the amplitude-damping channel (Fig. 5).

II. PRELIMINARIES

A. Quantum States and Channels

Let \mathcal{H} denote a Hilbert space, and $\mathcal{L}(\mathcal{H})$ be the set of bounded linear operators acting on \mathcal{H} . Denote by $\mathcal{L}_+(\mathcal{H})$ the subset of positive semi-definite operators of $\mathcal{L}(\mathcal{H})$. We define the Hilbert-Schmidt inner product between two linear operators $A, B \in \mathcal{L}(\mathcal{H})$ to be $\langle A, B \rangle := \text{Tr}[A^\dagger B]$. The state of a physical system is described by a density matrix $\rho \in \mathcal{D}(\mathcal{H})$, where $\mathcal{D}(\mathcal{H})$ is the subset of

positive semi-definite linear operators $\mathcal{L}_+(\mathcal{H})$ that have unit trace.

A linear map from $\mathcal{L}(\mathcal{H}^A)$ to $\mathcal{L}(\mathcal{H}^B)$ is denoted by $\mathcal{Q}^{A \rightarrow B} : \mathcal{L}(\mathcal{H}^A) \rightarrow \mathcal{L}(\mathcal{H}^B)$. We say that a linear map is positive if $\mathcal{Q}^{A \rightarrow B}(L_A) \in \mathcal{L}_+(\mathcal{H}^B)$ for all $L_A \in \mathcal{L}_+(\mathcal{H}^A)$, and trace preserving (TP) if $\text{Tr}[\mathcal{Q}^{A \rightarrow B}(L_A)] = \text{Tr}[L_A]$ for all $L_A \in \mathcal{L}(\mathcal{H}^A)$. A positive linear map $\mathcal{Q}^{A \rightarrow B}$ is called completely positive (CP) if for every Hilbert space \mathcal{H}^R , the map $id^R \otimes \mathcal{Q}^{A \rightarrow B}$ is positive, where id^R is the identity map acting on $\mathcal{L}(\mathcal{H}^R)$. For any $\mathcal{Q}^{A \rightarrow B}$ and $\mathcal{S}^{B \rightarrow C}$ linear maps, their composition is defined to be $(\mathcal{S} \circ \mathcal{Q})^{A \rightarrow C}(L_A) := \mathcal{S}(\mathcal{Q}(L_A))$, for all $L_A \in \mathcal{L}(\mathcal{H}^A)$. We define the adjoint map $(\mathcal{Q}^{A \rightarrow B})^\dagger$ of a linear map $\mathcal{Q}^{A \rightarrow B}$ with respect to the Hilbert-Schmidt inner product as $\langle \mathcal{Q}^{A \rightarrow B}(N_A), M_B \rangle = \langle N_A, (\mathcal{Q}^{A \rightarrow B})^\dagger(M_B) \rangle$ for all $N_A \in \mathcal{L}(\mathcal{H}^A)$ and $M_B \in \mathcal{L}(\mathcal{H}^B)$. More explicitly, if $\{Q_i\}_{i=1}^K$ are the Kraus operators of the CP map $\mathcal{Q}^{A \rightarrow B}$ (see Eq. (2)), then the Kraus operators of the adjoint map $(\mathcal{Q}^{A \rightarrow B})^\dagger$ are given by $\{Q_i^\dagger\}_{i=1}^K$.

The Choi Matrix of any linear map $\mathcal{Q}^{A \rightarrow B}$ is defined to be

$$\Gamma_{RB}^Q := id^R \otimes \mathcal{Q}^{A \rightarrow B}(|\Gamma\rangle\langle\Gamma|_{RA}), \quad (1)$$

where $|\Gamma\rangle_{RA} := \sum_{i=0}^{d-1} |i\rangle_R |i\rangle_A$ is the unnormalized maximally entangled state, with $d \equiv \dim \mathcal{H}^A = \dim \mathcal{H}^R$. The corresponding Choi state is defined as $\Phi_{RB}^Q := \Gamma_{RB}^Q/d$. The linear map $\mathcal{Q}^{A \rightarrow B}$ is TP if and only if its Choi matrix satisfies $\text{Tr}_B[\Gamma_{RB}^Q] = I_R$, and CP if and only if its Choi matrix is positive, i.e. $\Gamma_{RB}^Q \geq 0$.

In what follows, we suppress the system subscript and/or superscript if it does not lead to ambiguities. Every CP map $\mathcal{Q}^{A \rightarrow B}$ admits a Kraus decomposition

$$\mathcal{Q}(\cdot) = \sum_{i=1}^K Q_i(\cdot) Q_i^\dagger, \quad (2)$$

in terms of Kraus operators $\{Q_i\}_{i=1}^K$. If $\mathcal{Q}^{A \rightarrow B}$ is also TP, then $\sum_{i=1}^K Q_i^\dagger Q_i = I_A$ holds.

B. Quantum Fidelities

Given any two quantum states $\rho, \sigma \in \mathcal{D}(\mathcal{H})$ with $\dim \mathcal{H} \equiv d$, we define the fidelity function as follows

$$F(\rho, \sigma) := \left(\text{Tr} \left[\sqrt{\sqrt{\rho} \sigma \sqrt{\rho}} \right] \right)^2 = \|\sqrt{\rho} \sqrt{\sigma}\|_1^2. \quad (3)$$

If one of the two state, say $\sigma \equiv |\psi\rangle\langle\psi|$, is pure, then we have $F(\rho, \psi) = \langle\psi|\rho|\psi\rangle$. Based on this definition, various fidelities that are relevant in QEC and other areas of quantum information have been defined. One such quantity is called entanglement fidelity F_e of a channel $\mathcal{Q}^A \equiv \mathcal{Q}^{A \rightarrow A}$ with respect to a state $\rho \in \mathcal{D}(\mathcal{H}^A)$ [1, 2],

which is given by

$$F_e(\mathcal{Q}, \rho) := F(id^R \otimes \mathcal{Q}^A(\psi_{RA}^\rho), \psi_{RA}^\rho) \quad (4)$$

$$= \langle \psi^\rho | id^R \otimes \mathcal{Q}^A(\psi_{RA}^\rho) | \psi^\rho \rangle_{RA}, \quad (5)$$

where $\psi_{RA}^\rho \in \mathcal{H}^R \otimes \mathcal{H}^A$ is a purification of the density matrix $\rho \in \mathcal{D}(\mathcal{H}^A)$, i.e. $\text{Tr}_R \psi_{RA}^\rho = \rho_A$. It can be shown that the entanglement fidelity is independent of the particular choice of the purification, following from the fact that the former can be expressed in terms of the Kraus operators of \mathcal{Q}^A as [1, 2]

$$F_e(\mathcal{Q}, \rho) = \sum_{i=1}^K \text{Tr}[\rho Q_i] \text{Tr}[\rho Q_i^\dagger] = \sum_{i=1}^K |\text{Tr}[\rho Q_i]|^2. \quad (6)$$

The entanglement fidelity of a quantum channel \mathcal{Q}^A is defined to be the entanglement fidelity of \mathcal{Q}^A with respect to the maximally mixed state $\rho_A = I_A/d$ [29] (which is purified by the maximally entangled state $|\Phi\rangle_{RA}$). This can also be written in terms of the Choi state of \mathcal{Q}^A , as follows

$$F_e(\mathcal{Q}) \equiv F_e \left(\mathcal{Q}, \frac{I}{d} \right) \quad (7)$$

$$= \langle \Phi | id^R \otimes \mathcal{Q}^A(\Phi_{RA}) | \Phi \rangle_{RA} \quad (8)$$

$$= \langle \Phi | \Phi_{RA}^{\mathcal{Q}} | \Phi \rangle_{RA} \quad (9)$$

$$= F(\Phi^{\mathcal{Q}}, \Phi). \quad (10)$$

Another important fidelity measure of the form $F(\rho, \psi) = \langle \psi | \rho | \psi \rangle$ is the average channel (gate) fidelity $F_{\text{avg}}(\mathcal{Q})$, defined for $\forall |\psi\rangle \in \mathcal{H}^A$ and CPTP map \mathcal{Q}^A as

$$F_{\text{avg}}(\mathcal{Q}) := \int d\psi \langle \psi | \mathcal{Q}(\psi) | \psi \rangle, \quad (11)$$

where the discrete version has appeared in [1, 2]. In [30], the authors have shown that the average and entanglement fidelities are related by

$$F_{\text{avg}}(\mathcal{Q}) = \frac{dF_e(\mathcal{Q}) + 1}{d + 1}. \quad (12)$$

Finally, in what follows, we also use the simplifying notation

$$\delta^{\mathcal{Q}} := \arccos \sqrt{F_e(\mathcal{Q})}, \quad (13)$$

which can be interpreted in the χ -matrix representation of quantum channels as the “error angle” by which the Kraus operators of the noisy channel \mathcal{Q} deviate from the desired “no error” normalized basis element $B_0 = I/\sqrt{d}$ (where $\langle B_0, B_0 \rangle = 1$) of the d^2 dimensional vector space $\mathcal{L}(\mathcal{H})$ (see Appendix A for details). It turns out that the error angle notation is very convenient when expressing the average fidelity of composite channels in terms of the individual average channel fidelities [27].

C. Channel Twirlings

Twirling of quantum channels plays an important role in QEC and fault-tolerant quantum computing [31–37]. Examples include: (1) similarities between QEC codes for channels and their twirled versions [32], (2) the simulability of twirled quantum channels on a quantum computer, due to the Gottesman-Knill theorem [38], (3) the fact that channels and their twirled versions share the same average and entanglement fidelities [30], (4) various twirlings (Pauli, Clifford, and uniform Haar) rendering channels depolarizing [30, 35, 36, 39], (5) and finally, their close connection to unitary t -designs. Due to its importance, I recall some relevant properties of unitary t -designs in Appendix B (also see [33, 40] for a brief review).

Generally, channel twirlings can be defined with respect to both discrete and continuous sets of unitaries. In its most simple form, for a set of unitaries $\{U_A(x), V_B(x)\}_{x \in \mathcal{X}}$ and a probability distribution function p_X defined over a finite set \mathcal{X} , the twirling of a quantum channel $\mathcal{Q}^{A \rightarrow B}$ (which we denote by a tilde symbol $\tilde{\mathcal{Q}}^{A \rightarrow B}$) is defined as

$$\tilde{\mathcal{Q}}^{A \rightarrow B} := \sum_{x \in \mathcal{X}} p_X(x) \mathcal{V}_x^{B\dagger} \circ \mathcal{Q}^{A \rightarrow B} \circ \mathcal{U}_x^A, \quad (14)$$

where we have used the notation for the unitary channels $\mathcal{U}_x^A(\cdot) := U_A^\dagger(x)(\cdot)U_A(x)$ and $\mathcal{V}_x^B(\cdot) := V_B^\dagger(x)(\cdot)V_B(x)$, for $\forall x \in \mathcal{X}$. Although most of the results presented in this article are valid for any finite set \mathcal{X} , the case where it forms a group and $\{U_A(x), V_B(x)\}_{x \in \mathcal{X}}$ two unitary representations of it are of great interest [41] (see Remark 2).

Twirlings with continuous sets of unitaries have also been studied extensively in literature. If we have some probability distribution (measure) $\mu(U)$ over the set of $d \times d$ unitary matrices $\mathbb{U}(d)$, then the continuous twirling of the channel \mathcal{Q}^A is defined to be

$$\tilde{\mathcal{Q}} := \int_{\mathbb{U}(d)} d\mu(U) \mathcal{U}^\dagger \circ \mathcal{Q} \circ \mathcal{U}. \quad (15)$$

D. Generalized Distinguishability and Distance Measures

To quantify the success of a recovery protocol (such as QEC), we need to introduce the concepts of a generalized distinguishability and distance measures between two states as well as between two channels [41–46].

We say that $\mathbf{D} : \mathcal{D}(\mathcal{H}) \times \mathcal{L}_+(\mathcal{H}) \rightarrow \mathbb{R}^1$ is a generalized distinguishability measure between two states if it satisfies the *data-processing inequality* (DPI), i.e. for arbitrary \mathcal{Q} CPTP map and $\forall \rho, \sigma \in \mathcal{D}(\mathcal{H})$, we have [47]

$$\mathbf{D}(\mathcal{Q}(\rho), \mathcal{Q}(\sigma)) \leq \mathbf{D}(\rho, \sigma). \quad (16)$$

An important consequence of DPI is the property of iso-

metric invariance. Namely, for any isometry V , the following holds [46]

$$\mathbf{D}(\mathcal{V}(\rho), \mathcal{V}(\sigma)) = \mathbf{D}(\rho, \sigma), \quad (17)$$

where $\mathcal{V}(\cdot) = V^\dagger(\cdot)V$.

Independently, we say that $\mathbf{D} : \mathcal{D}(\mathcal{H}) \times \mathcal{D}(\mathcal{H}) \rightarrow \mathbb{R}_+^1$ is a generalized distance measure between two states if it satisfies the following three properties for $\forall \rho, \sigma, \tau \in \mathcal{D}(\mathcal{H})$:

1. *Positivity and faithfulness*:

$$\mathbf{D}(\rho, \sigma) \geq 0, \quad (18)$$

where the equality holds iff $\rho = \sigma$.

2. *Symmetry*: $\mathbf{D}(\rho, \sigma) = \mathbf{D}(\sigma, \rho)$.

3. *Triangle inequality*:

$$\mathbf{D}(\rho, \sigma) \leq \mathbf{D}(\rho, \tau) + \mathbf{D}(\tau, \sigma). \quad (19)$$

A common requirement for fault-tolerant QEC and quantum computing is the so-called “chaining property” [42, 44]. However, this property of generalized distinguishability/distance measures is derivative from more elementary properties, such as DPI and the triangle inequality (see Appendix C for a short discussion).

Finally, we say that the map $\mathbf{D} : \mathcal{D}(\mathcal{H}) \times \mathcal{L}_+(\mathcal{H}) \rightarrow \mathbb{R}_+^1$ satisfies the *joint convexity* property if for any two ensembles $\{p_X(x), \rho^x\}_{x \in \mathcal{X}}$ and $\{p_X(x), \sigma^x\}_{x \in \mathcal{X}}$, where p_X is a probability distribution function of the random variable X over the set \mathcal{X} , we have

$$\mathbf{D} \left(\sum_{x \in \mathcal{X}} p_X(x) \rho^x, \sum_{x \in \mathcal{X}} p_X(x) \sigma^x \right) \leq \sum_{x \in \mathcal{X}} p_X(x) \mathbf{D}(\rho^x, \sigma^x). \quad (20)$$

For fidelity based distinguishability measures, such as the Bures and Sine distances, this directly follows from the double concavity of the fidelity function (see e.g. [46]).

Alternatively, it is well-known that the joint convexity property can be derived from the DPI (with respect to the partial trace channel) if we further assume that \mathbf{D} satisfies the direct sum property for classical-quantum states [46], i.e.

$$\begin{aligned} \mathbf{D} \left(\sum_{x \in \mathcal{X}} p_X(x) |x\rangle\langle x| \otimes \rho^x, \sum_{x \in \mathcal{X}} p_X(x) |x\rangle\langle x| \otimes \sigma^x \right) \\ = \sum_{x \in \mathcal{X}} p_X(x) \mathbf{D}(\rho^x, \sigma^x). \end{aligned} \quad (21)$$

For a summary of various distinguishability and/or distance measures, as well as which properties they satisfy, please see Table I. All the above properties are satisfied by [44, 46]

1. Trace Distance: $\mathbf{D}_{\text{Tr}}(\rho, \sigma) = \frac{1}{2} \|\rho - \sigma\|_1$.

2. Bures Distance: $\mathbf{D}_B(\rho, \sigma) = \sqrt{2 - 2\sqrt{F(\rho, \sigma)}}$.

3. Sine Distance: $\mathbf{D}_S(\rho, \sigma) = \sqrt{1 - F(\rho, \sigma)}$,

where $F(\rho, \sigma) = \|\sqrt{\rho}\sqrt{\sigma}\|_1^2$ is the fidelity function.

Using the generalized distinguishability (distance) measures between two states, we define the generalized distinguishability (distance) measures between two channels $\mathcal{Q}^{A \rightarrow B}$ and $\mathcal{S}^{A \rightarrow B}$, as follows

$$\mathbf{D}(\mathcal{Q}, \mathcal{S}) := \sup_{\rho} \mathbf{D}(id^R \otimes \mathcal{Q}^{A \rightarrow B}(\rho), id^R \otimes \mathcal{S}^{A \rightarrow B}(\rho)), \quad (22)$$

where $\rho \in \mathcal{D}(\mathcal{H}^A \otimes \mathcal{H}^R)$, for arbitrary Hilbert space dimensions of the reference system R . By using joint convexity and the Schmidt decomposition of pure states, it can be shown that the maximization need only be taken over pure states ψ_{RA} , with the reference system R having the same Hilbert space dimensions as A [46], i.e.

$$\mathbf{D}(\mathcal{Q}, \mathcal{S}) := \sup_{\psi} \mathbf{D}(id^R \otimes \mathcal{Q}^{A \rightarrow B}(\psi), id^R \otimes \mathcal{S}^{A \rightarrow B}(\psi)). \quad (23)$$

Finally, it is important to note that the joint convexity property of generalized distinguishability measures for states implies the same property for channels. This is seen by considering the two channels $\mathcal{Q}^{A \rightarrow B} = \sum_{x \in \mathcal{X}} p_X(x) \mathcal{Q}_x^{A \rightarrow B}$ and $\mathcal{S}^{A \rightarrow B} = \sum_{x \in \mathcal{X}} p_X(x) \mathcal{S}_x^{A \rightarrow B}$, and then applying the joint convexity property for states, as follows

$$\begin{aligned} \mathbf{D}(\mathcal{Q}, \mathcal{S}) &= \sup_{\rho} \mathbf{D}(id^R \otimes \mathcal{Q}^{A \rightarrow B}(\rho), id^R \otimes \mathcal{S}^{A \rightarrow B}(\rho)) \\ &\quad (24) \end{aligned}$$

$$= \mathbf{D}(id^R \otimes \mathcal{Q}^{A \rightarrow B}(\rho^*), id^R \otimes \mathcal{S}^{A \rightarrow B}(\rho^*)) \quad (25)$$

$$\leq \sum_{x \in \mathcal{X}} p_X(x) \mathbf{D}(id^R \otimes \mathcal{Q}_x^{A \rightarrow B}(\rho^*), id^R \otimes \mathcal{S}_x^{A \rightarrow B}(\rho^*)) \quad (26)$$

$$\leq \sum_{x \in \mathcal{X}} p_X(x) \sup_{\rho} \mathbf{D}(id^R \otimes \mathcal{Q}_x^{A \rightarrow B}(\rho), id^R \otimes \mathcal{S}_x^{A \rightarrow B}(\rho)) \quad (27)$$

$$\equiv \sum_{x \in \mathcal{X}} p_X(x) \mathbf{D}(\mathcal{Q}_x, \mathcal{S}_x). \quad (28)$$

Consequently, we have the joint convexity property

$$\begin{aligned} \mathbf{D} \left(\sum_{x \in \mathcal{X}} p_X(x) \mathcal{Q}_x, \sum_{x \in \mathcal{X}} p_X(x) \mathcal{S}_x \right) \\ \leq \sum_{x \in \mathcal{X}} p_X(x) \mathbf{D}(\mathcal{Q}_x, \mathcal{S}_x). \end{aligned} \quad (29)$$

III. LOWER-BOUNDING GENERALIZED DISTINGUISHABILITY MEASURES

We start this section by showing a simple property that all generalized distinguishability measures satisfy with re-

List of different measures			
Name	Data Processing	Distance Measure	joint convexity
Quantum Relative Entropy	Yes	No	Yes
Generalized α -Relative Entropies (Petz-Renyi, Sandwiched, etc.)	Yes	No	Yes
Trace Distance	Yes	Yes	Yes
Bures Distance	Yes	Yes	Yes
Sine Distance	Yes	Yes	Yes
Amortized Divergence [48]	Yes	No	Yes

TABLE I. Summary of properties of various measures used in quantum information theory.

spect to channel twirling, if the joint convexity property (or equivalently, if the direct sum property) is further assumed.

Lemma 1. *Assume that we are given two CPTP maps $\mathcal{Q}^{A \rightarrow B}$ and $\mathcal{S}^{A \rightarrow B}$, a set of unitaries $\{U_A(x), V_B(x)\}_{x \in \mathcal{X}}$, and a probability distribution function p_X defined over the finite set \mathcal{X} . If the generalized distinguishability measure \mathbf{D} satisfies the joint convexity property, then $\mathbf{D}(\mathcal{Q}, \mathcal{S})$ is lower bounded by the generalized distinguishability measure between the corresponding twirled channels $\tilde{\mathcal{Q}}^{A \rightarrow B}$ and $\tilde{\mathcal{S}}^{A \rightarrow B}$ with respect to the given weighted set of unitaries above, as follows*

$$\mathbf{D}(\mathcal{Q}, \mathcal{S}) \geq \mathbf{D}(\tilde{\mathcal{Q}}, \tilde{\mathcal{S}}), \quad (30)$$

where the lower bound is saturated iff the joint convexity of the generalized distinguishability measure between the two quantum channels is saturated with respect to the above set of weighted unitaries.

Proof. Consider the isometric invariance property of $\mathbf{D}(\mathcal{Q}, \mathcal{S})$, namely for any $\mathcal{U} := U(\cdot)U^\dagger$, where $U \in \mathbf{U}(d)$, we have

$$\mathbf{D}(\mathcal{Q}, \mathcal{S}) = \mathbf{D}(\mathcal{U} \circ \mathcal{Q}, \mathcal{U} \circ \mathcal{S}) \quad (31)$$

$$= \mathbf{D}(\mathcal{Q} \circ \mathcal{U}, \mathcal{S} \circ \mathcal{U}), \quad (32)$$

where the first equality follows from Eq. (17) and the second equality follows from the definition in Eq. (22). This implies that for $\forall U_A \in \mathbf{U}(d_A)$ and $\forall V_B \in \mathbf{U}(d_B)$

$$\mathbf{D}(\mathcal{Q}, \mathcal{S}) = \mathbf{D}(\mathcal{V}^\dagger \circ \mathcal{Q} \circ \mathcal{U}, \mathcal{V}^\dagger \circ \mathcal{S} \circ \mathcal{U}). \quad (33)$$

Consequently, by considering the generalized distinguishability measure $\mathbf{D}(\tilde{\mathcal{Q}}, \tilde{\mathcal{S}})$ between the twirled channels, we arrive at

$$\mathbf{D} \left(\sum_{x \in \mathcal{X}} p_X(x) \mathcal{V}^{x\dagger} \circ \mathcal{Q} \circ \mathcal{U}^x, \sum_{x \in \mathcal{X}} p_X(x) \mathcal{V}^{x\dagger} \circ \mathcal{S} \circ \mathcal{U}^x \right) \quad (34)$$

$$\leq \sum_{x \in \mathcal{X}} p_X(x) \mathbf{D}(\mathcal{V}^{x\dagger} \circ \mathcal{Q} \circ \mathcal{U}^x, \mathcal{V}^{x\dagger} \circ \mathcal{S} \circ \mathcal{U}^x) \quad (35)$$

$$= \sum_{x \in \mathcal{X}} p_X(x) \mathbf{D}(\mathcal{Q}, \mathcal{S}) = \mathbf{D}(\mathcal{Q}, \mathcal{S}), \quad (36)$$

where the inequality follows from Eq. (29). \blacksquare

Remark 1. *This lemma can be viewed as a special case of a more general result for quantum supermaps. To elaborate, we recall that a supermap (a linear map from one quantum channel to another) can always be expressed as a pre and post-processing maps concatenated with the input quantum channel, and assisted by a memory [49]. Then, Lemma 1 follows from applying the data-processing inequality for generalized distinguishability measures between two quantum channels [50] with respect to channel twirling, which is a valid quantum supermap.*

Remark 2. *In [41], the authors have shown that for any two covariant channels $\mathcal{F}^{A \rightarrow B}$ and $\mathcal{G}^{A \rightarrow B}$ with respect to $\{U_A(x), V_B(x)\}_{x \in \mathcal{X}}$ (namely that $\mathcal{V}_x \circ \mathcal{F} = \mathcal{F} \circ \mathcal{U}_x$ for $\forall x \in \mathcal{X}$, and similarly for \mathcal{G}), the generalized distinguishability measure*

$$\mathbf{D}(\mathcal{F}, \mathcal{G}) = \sup_{\phi} \mathbf{D}((id \otimes \mathcal{F})(\phi_{RA}), (id \otimes \mathcal{G})(\phi_{RA})), \quad (37)$$

can be found by maximizing only over symmetric states ϕ_{RA} , defined as

$$\frac{1}{|\mathcal{X}|} \sum_{x \in \mathcal{X}} U_A^\dagger(x) \phi_{RA} U_A(x) = \phi_{RA}. \quad (38)$$

However, since the twirlings $\mathcal{F} \equiv \tilde{\mathcal{Q}}$ and $\mathcal{G} \equiv \tilde{\mathcal{S}}$ in Lemma 1 are trivially covariant with respect to the unitary representations $\{U_A(x), V_B(x)\}_{x \in \mathcal{X}}$ of the finite group \mathcal{X} , this implies that the lower bound in Eq. (30) need only be computed for such symmetric states. Furthermore, if $\{U_A(x)\}_{x \in \mathcal{X}}$ is a unitary 1-design (i.e. it is an irreducible representation of the group \mathcal{X} of degree d_A), then, using the property Eq. (B2) of unitary 1-designs, the maximization is found by computing the generalized distinguishability measure exactly for the maximally entangled state

$$\mathbf{D}(\tilde{\mathcal{Q}}, \tilde{\mathcal{S}}) = \mathbf{D}((id^R \otimes \tilde{\mathcal{Q}}^A)(\Phi_{RA}), (id^R \otimes \tilde{\mathcal{S}}^A)(\Phi_{RA})). \quad (39)$$

So far, we have shown that the generalized distinguishability measure between $\mathcal{Q}^{A \rightarrow B}$ and $\mathcal{S}^{A \rightarrow B}$ is lower bounded by the corresponding distinguishability measure for arbitrary discrete twirlings of these channels. We now

show that a similar lower bound can be derived for the uniform Haar twirling. But first, we recall the following important result

Lemma 2. ([30]) *Given a CPTP map $\mathcal{Q}^{A \rightarrow A}$ and $\forall \rho \in \mathcal{D}(\mathcal{H}^A)$, the continuous twirling $\tilde{\mathcal{Q}} = \int_{\mathbf{U}(d)} dU \mathcal{U}^\dagger \circ \mathcal{Q} \circ \mathcal{U}$ over the uniform Haar measure on the set of $d \times d$ unitary matrices $\mathbf{U}(d)$ is given by the depolarizing channel*

$$\tilde{\mathcal{Q}}(\rho) = (1 - p^{\mathcal{Q}})\rho + p^{\mathcal{Q}} \frac{I}{d}, \quad (40)$$

where the depolarizing parameter $p^{\mathcal{Q}}$ is given by the average fidelity of \mathcal{Q} , as follows

$$p^{\mathcal{Q}} = \frac{d}{d-1} (1 - F_{\text{avg}}(\mathcal{Q})). \quad (41)$$

The proof of Eq. (40) is shown in [30, 39] for some parameter value $p^{\mathcal{Q}}$. Eq. (41) is a direct consequence of the fact that the uniform Haar twirled channel $\tilde{\mathcal{Q}} = \int_{\mathbf{U}(d)} dU \mathcal{U}^\dagger \circ \mathcal{Q} \circ \mathcal{U}$ has the same average fidelity as the original channel \mathcal{Q} [30], along with the fact that the average fidelity of the depolarizing channel is given by

$$F_{\text{avg}}(\tilde{\mathcal{Q}}) = 1 - \left(\frac{d-1}{d} \right) p, \quad (42)$$

where we have used the normalization $\int d\psi = 1$ and the notation p for the depolarizing parameter.

Using the above Lemmas 1 and 2, we now establish a similar lower bound to that in Lemma 1 for the uniform Haar twirl.

Theorem 1. *Assume that we are given two CPTP maps $\mathcal{Q}^{A \rightarrow A}$ and $\mathcal{S}^{A \rightarrow A}$. If the generalized distinguishability measure \mathbf{D} satisfies the joint convexity property, then $\mathbf{D}(\mathcal{Q}, \mathcal{S})$ is lower bounded by some function $l_{\mathbf{D}}$ of the channel entanglement fidelities $F_e(\mathcal{Q})$ and $F_e(\mathcal{S})$, as follows*

$$\mathbf{D}(\mathcal{Q}, \mathcal{S}) \geq l_{\mathbf{D}}(F_e(\mathcal{Q}), F_e(\mathcal{S})), \quad (43)$$

where the specific form of the function $l_{\mathbf{D}}$ depends on the choice of the generalized distinguishability measure and is determined by the uniform Haar twirls, as follows

$$l_{\mathbf{D}}(F_e(\mathcal{Q}), F_e(\mathcal{S})) \equiv \mathbf{D}(\tilde{\mathcal{Q}}, \tilde{\mathcal{S}}), \quad (44)$$

where $\tilde{\mathcal{Q}} = \int_{\mathbf{U}(d)} dU \mathcal{U}^\dagger \circ \mathcal{Q} \circ \mathcal{U}$ and $\tilde{\mathcal{S}} = \int_{\mathbf{U}(d)} dU \mathcal{U}^\dagger \circ \mathcal{S} \circ \mathcal{U}$ yield two depolarizing channels. The inequality is saturated if the joint convexity property is saturated for a set of unitary 2-designs and a uniform probability distribution over this set.

Proof. This is a direct consequence of applying Lemma 1 to any unitary 2-design $\{U_A(x)\}_{x \in \mathcal{X}}$, e.g. the unitary representation of the Clifford group (see Appendix B), along with a uniform distribution on \mathcal{X} , and then using the property of unitary 2-designs in Eq. (B4), which

finally yields

$$\mathbf{D}(\mathcal{Q}, \mathcal{S}) \geq \mathbf{D}(\tilde{\mathcal{Q}}, \tilde{\mathcal{S}}), \quad (45)$$

where $\tilde{\mathcal{Q}} = \int_{\mathbf{U}(d)} dU \mathcal{U}^\dagger \circ \mathcal{Q} \circ \mathcal{U}$ and $\tilde{\mathcal{S}} = \int_{\mathbf{U}(d)} dU \mathcal{U}^\dagger \circ \mathcal{S} \circ \mathcal{U}$. The proof is completed by applying Lemma 2 and plugging in the depolarizing channels into the lower bound in Eq. (45). ■

It directly follows from this proof that the image of the function $l_{\mathbf{D}}$ coincides with the image of the corresponding generalized distinguishability measure \mathbf{D} .

Remark 3. *The lower bound proof does not require faithfulness, symmetry, nor the triangle inequality, which would also make \mathbf{D} a generalized distance measure. However, the triangle inequality becomes necessary when deriving an upper bound for the generalized distinguishability measure for concatenated noisy channels (or gates), as it is relevant to fault-tolerant quantum computing (see Appendix D for more details).*

IV. LOWER-BOUNDING DIAMOND DISTANCE USING ENTANGLEMENT FIDELITY

We now consider the diamond distance as an important example of a generalized distinguishability measure and derive a lower bound using the entanglement fidelity difference between the two channels of interest. The diamond distance is relevant due to two important facts: (1) it has a clear operational meaning in terms of the maximum probability of distinguishing between two channels in a quantum channel discrimination task [51] and (2) it satisfies the triangle inequality and hence also the chaining property, which is useful for bounding errors in fault-tolerant quantum computing (see Appendix C).

In this section, I present a consequence of Theorem 1 that will prove useful for determining the role of incomplete knowledge in recovery protocols. But first, let us analytically compute the lower bound in Theorem 1 for the diamond distance.

Lemma 3. *For any two depolarizing channels $\tilde{\mathcal{Q}}^{A \rightarrow A}$ and $\tilde{\mathcal{S}}^{A \rightarrow A}$, the diamond distance between them is equal to the difference between their entanglement fidelities, namely*

$$\frac{1}{2} \|\tilde{\mathcal{Q}} - \tilde{\mathcal{S}}\|_{\diamond} = |F_e(\tilde{\mathcal{Q}}) - F_e(\tilde{\mathcal{S}})|. \quad (46)$$

Proof. Assume that $\tilde{\mathcal{Q}}$ and $\tilde{\mathcal{S}}$ are depolarizing channels with depolarizing parameters $p^{\mathcal{Q}}$ and $p^{\mathcal{S}}$, respectively. Namely,

$$\tilde{\mathcal{Q}}^A = (1 - p^{\mathcal{Q}})id^A + p^{\mathcal{Q}} \frac{I_A}{d_A} \text{Tr}_A, \quad (47)$$

$$\tilde{\mathcal{S}}^A = (1 - p^{\mathcal{S}})id^A + p^{\mathcal{S}} \frac{I_A}{d_A} \text{Tr}_A, \quad (48)$$

and hence

$$id^R \otimes \tilde{\mathcal{Q}}^A = (1 - p^{\mathcal{Q}})id^{RA} + p^{\mathcal{Q}}\text{Tr}_A \otimes \frac{I_A}{d_A}, \quad (49)$$

$$id^R \otimes \tilde{\mathcal{S}}^A = (1 - p^{\mathcal{S}})id^{RA} + p^{\mathcal{S}}\text{Tr}_A \otimes \frac{I_A}{d_A}, \quad (50)$$

yields for the diamond distance

$$\frac{1}{2}\|\tilde{\mathcal{Q}} - \tilde{\mathcal{S}}\|_{\diamond} = \kappa |p^{\mathcal{S}} - p^{\mathcal{Q}}| \quad (51)$$

$$= \frac{d\kappa}{d-1} |F_{\text{avg}}(\tilde{\mathcal{Q}}) - F_{\text{avg}}(\tilde{\mathcal{S}})| \quad (52)$$

$$= \frac{d^2\kappa}{d^2-1} |F_e(\tilde{\mathcal{Q}}) - F_e(\tilde{\mathcal{S}})|, \quad (53)$$

where

$$\kappa(d) \equiv \frac{1}{2} \sup_{\psi_{RA}} \left\| \psi_{RA} - \rho_R \otimes \frac{I_A}{d_A} \right\|_1, \quad (54)$$

and we have used Eq. (12). We can rewrite κ using the diamond distance between the identity and the replacement channel, as follows

$$\kappa(d) = \frac{1}{2} \left\| id^A - \frac{I_A}{d} \text{Tr}_A \right\|_{\diamond}. \quad (55)$$

Next, we use the semi-definite program for the normalized diamond norm [52]

$$\frac{1}{2} \left\| id^A - \frac{I_A}{d} \text{Tr}_A \right\|_{\diamond} \quad (56)$$

$$= \sup_{\sigma_{RA}, \rho_R} \text{Tr}_{RA} \left[\sigma_{RA} \left(\Gamma_{RA}^{id} - \Gamma_{RA}^{\frac{I_A}{d} \text{Tr}_A} \right) \right] \quad (57)$$

$$= \sup_{\sigma_{RA}, \rho_R} \text{Tr}_{RA} \left[\sigma_{RA} \left(\Gamma_{RA} - \frac{I_{RA}}{d} \right) \right], \quad (58)$$

where the supremum is taken over all positive matrices $0 \leq \sigma_{RA} \leq \rho_R \otimes I_A$, and $\rho_R \in \mathcal{D}(\mathcal{H}^R)$. Consider the eigenvalues of the $d^2 \times d^2$ matrix $\Gamma_{RA} - I_{RA}/d$. First, if we denote some fixed eigenvalue of Γ_{RA} by γ , then the corresponding eigenvalue of $\Gamma_{RA} - I_{RA}/d$ is $\gamma - 1/d$. Next, let us show that $d^2 - 1$ of the d^2 eigenvalues of Γ_{RA} are zero. This follows by considering the kernel space of Γ_{RA} (the zero eigenvalue subspace), denoted by $\text{ker}(\Gamma_{RA}) \subset \mathcal{H}^R \otimes \mathcal{H}^A$. Namely, for $\forall |\psi\rangle_{RA} \in \text{ker}(\Gamma_{RA})$ we have, by definition, $\Gamma_{RA}|\psi\rangle_{RA} = 0$. This is true for all states $|\psi\rangle_{RA}$ for which $\langle \Gamma | \psi \rangle_{RA} = 0$, i.e. $|\psi\rangle_{RA} \in (\text{span}\{|\Gamma\rangle\})^{\perp}$, which is the $(d^2 - 1)$ -dimensional orthogonal complement of the one-dimensional subspace $\text{span}\{|\Gamma\rangle\} \subset \mathcal{H}^R \otimes \mathcal{H}^A$. Finally, we note that the only non-zero eigenvalue γ_0 of Γ_{RA} is determined by the trace $\text{Tr}_{RA}[\Gamma_{RA}] = d$, and hence $\gamma_0 = d$. Therefore, the eigenvalues of $\Gamma_{RA} - I_{RA}/d$

are given by the list

$$\text{eigenval} \left(\Gamma - \frac{I}{d} \right) = \left\{ \frac{d^2 - 1}{d}, -\frac{1}{d}, -\frac{1}{d}, \dots, -\frac{1}{d} \right\}. \quad (59)$$

As we can see, only one of the eigenvalues of $\Gamma_{RA} - I_{RA}/d$ is positive. Therefore, we write the spectral decomposition of the matrix $\Gamma_{RA} - I_{RA}/d$ as follows

$$\Gamma_{RA} - \frac{I_{RA}}{d} = \frac{d^2 - 1}{d} |\gamma_0\rangle\langle\gamma_0| - \frac{1}{d} \sum_{i=1}^{d^2-1} |\gamma_i\rangle\langle\gamma_i|, \quad (60)$$

where $\{|\gamma_i\rangle\}_{i=0}^{d^2-1}$ is its set of orthonormal eigenbasis.

It follows that, to maximize the argument of Eq. (58), we need to consider the support of the positive semi-definite operator σ_{RA} to be in the (one-dimensional) support of Γ_{RA} (which is orthogonal to $\text{ker}(\Gamma_{RA})$), i.e. we need to search for σ_{RA} in the form $\sigma_{RA} = z|\gamma_0\rangle\langle\gamma_0|$ for some $z \geq 0$. Substituting into the constraint $\sigma_{RA} \leq \rho_R \otimes I_A$ gives

$$\rho_R \otimes I_A - z|\gamma_0\rangle\langle\gamma_0| \geq 0 \quad (61)$$

$$\Rightarrow \langle \Gamma | \rho_R \otimes I_A | \Gamma \rangle_{RA} - z|\langle \Gamma | \gamma_0 \rangle|^2 \geq 0 \quad (62)$$

$$\Rightarrow \text{Tr}[\rho] - z\langle \gamma_0 | \Gamma | \gamma_0 \rangle_{RA} \geq 0 \quad (63)$$

$$\Rightarrow 1 - zd \geq 0 \Rightarrow z \leq \frac{1}{d}. \quad (64)$$

Consequently, if $\exists \rho_R \in \mathcal{D}(\mathcal{H}^R)$ such that σ_{RA} is fully in the support of Γ_{RA} , i.e. $\sigma_{RA} = z|\gamma_0\rangle\langle\gamma_0|_{RA}$ (where $\Gamma|\gamma_0\rangle = d|\gamma_0\rangle$), then it must be the case that the normalization $z \leq 1/d$. The resulting maximization in Eq. (58) will thus yield for $\kappa(d)$

$$\sup_{\sigma_{RA}, \rho_R} \text{Tr}_{RA} \left[\sigma_{RA} \left(\Gamma_{RA} - \frac{I_{RA}}{d} \right) \right] = \frac{d^2 - 1}{d} z_{\max} \quad (65)$$

$$= \frac{d^2 - 1}{d^2}, \quad (66)$$

or equivalently,

$$\frac{1}{2} \|\tilde{\mathcal{Q}} - \tilde{\mathcal{S}}\|_{\diamond} = \frac{d^2\kappa(d)}{d^2-1} |F_e(\tilde{\mathcal{Q}}) - F_e(\tilde{\mathcal{S}})| \quad (67)$$

$$= |F_e(\tilde{\mathcal{Q}}) - F_e(\tilde{\mathcal{S}})|. \quad (68)$$

In the above analysis, we presumed the existence of a density matrix ρ_R for which $\sigma_{RA} = z|\gamma_0\rangle\langle\gamma_0|_{RA} \leq \rho_R \otimes I_A$. It is easy to see that the pick $\rho_R = I_R/d$ satisfies the inequality $z|\gamma_0\rangle\langle\gamma_0|_{RA} \leq \rho_R \otimes I_A$, as well as allowing the normalization z to reach its maximum value $z_{\max} = 1/d$.

Note that, if we extend the support $\sigma_{RA} = z|\gamma_0\rangle\langle\gamma_0| + \sum_{i=1}^{d^2-1} z_i|\gamma_i\rangle\langle\gamma_i|$, then the above argument (starting from Eq. (61)) still yields $z \leq 1/d$, while simultaneously leading to a sub-optimal outcome in Eq. (65) due to the contribution of the negative eigenvalues of $\Gamma_{RA} - I_{RA}/d$. Taking σ_{RA} to be off-diagonal in the $\{|\gamma_i\rangle\}_{i=0}^{d^2-1}$ does not change this argument. ■

It is important to note that this lemma has been known previously for special cases, e.g. in [25, 26] between qubit depolarizing maps ($d = 2$) and between a qudit depolarizing map and the identity map ($p^S = 0$), respectively. However, Pirandola *et al.* in [25] used a different technique to compute essentially the same quantity $\kappa(d)$ appearing in our derivation of Lemma 3, which crucially does not depend on the depolarizing parameters p^Q and p^S .

We are now ready to prove a general lower bound for the diamond distance between any two quantum channels with the same input and output spaces. We frame this as follows

Corollary 1. *For any two CPTP maps $\mathcal{Q}^{A \rightarrow A}$ and $\mathcal{S}^{A \rightarrow A}$, the diamond distance between them is lower bounded by the difference in their entanglement fidelities, namely*

$$\frac{1}{2} \|\mathcal{Q} - \mathcal{S}\|_{\diamond} \geq |F_e(\mathcal{Q}) - F_e(\mathcal{S})|. \quad (69)$$

where the inequality is saturated if the joint convexity property is saturated for a set of unitary 2-designs and a uniform probability distribution over this set.

Proof. We apply Theorem 1 to the diamond distance $\mathbf{D}(\mathcal{Q}, \mathcal{S}) \equiv \frac{1}{2} \|\mathcal{Q} - \mathcal{S}\|_{\diamond}$ and use Lemma 3 to compute the lower bound $l_{\diamond}(F_e(\mathcal{Q}), F_e(\mathcal{S})) \equiv \frac{1}{2} \|\tilde{\mathcal{Q}} - \tilde{\mathcal{S}}\|_{\diamond}$. The proof is completed by recalling that the entanglement fidelity of a quantum channel is preserved under uniform Haar twirling [30]. \blacksquare

V. FUNDAMENTAL BOUNDS ON RECOVERY WITH INCOMPLETE KNOWLEDGE

In this section, we are interested in the spectator-based recovery setting, which is succinctly described in Fig. 2. The goal is to achieve complete (or, at least, an approximate) recovery $\mathcal{R}_{\theta} \circ \mathcal{N}_{\theta}(\rho) = \rho$ of the noisy channel \mathcal{N}_{θ} for a subset of states $\rho \in \mathcal{D}(\mathcal{C}) \subset \mathcal{D}(\mathcal{H})$ in the codespace \mathcal{C} . The noisy channel \mathcal{N}_{θ} is picked from a parametric family of noisy channels $\{\mathcal{N}_{\theta}\}_{\theta \in \Theta}$ that is motivated from certain physical assumptions about the environment. The “optimality” of the recovery \mathcal{R}_{θ} for a given noisy channel \mathcal{N}_{θ} could be quantified in various ways. Motivated by Corollary 1, we choose the entanglement fidelity to be the quantifier of the optimal recovery, i.e.

$$\mathcal{R}_{\theta} := \operatorname{argmax} F_e(\mathcal{R} \circ \mathcal{N}_{\theta}); \mathcal{R} \in \text{CPTP}(\mathcal{H}). \quad (70)$$

Indeed, entanglement fidelity has been used as a measure of success of QEC in e.g. [6, 8, 29, 53–55]. In what follows, we consider two difference scenarios:

- *Optimal recovery scenario* (Fig. 1), which corresponds to the optimal choice of the recovery map \mathcal{R}_{θ} (as defined in Eq. (70)) for the noisy channel \mathcal{N}_{θ} , where the value of $\theta \in \Theta$ is completely known.

- *Best-guess recovery scenario* (Fig. 2), which corresponds to the optimal recovery choice $\mathcal{R}_{\hat{\theta}}$ (as defined in Eq. (70)) for the estimated noisy channel $\mathcal{N}_{\hat{\theta}}$, where $\hat{\theta}$ is the best estimate of θ .

Remark 4. *Not all QEC codes require a recovery channel \mathcal{R}_{θ} that depends on the noise parameter θ . Such channels are known to be Pauli channels, where the recovery operation is fully determined by a subset of Pauli operators from the general Pauli group, as is known in the stabilizer formalism of QEC [56, 57]. Therefore, in what follows, we consider non-Pauli channels, of which, the generalized amplitude damping channel is a prime example [57].*

A. Information-Theoretic Bounds

The results we derived in the previous section hold for any two quantum channels \mathcal{Q} and \mathcal{S} with the same input and output spaces. We now consider these results in the light of general single-cycle recovery protocols.

1. Fundamental Limitations for Perfect Knowledge Scenario

Assume that we are given a noise channel $\mathcal{N}^{A \rightarrow B}$. By picking $\mathcal{Q}^A \equiv \mathcal{R}^{B \rightarrow A} \circ \mathcal{N}^{A \rightarrow B}$ and $\mathcal{S}^A \equiv \text{id}^A$, Corollary 1 can be reframed in the context of noise recovery to read:

Corollary 2. *Given a noisy channel $\mathcal{N}^{A \rightarrow B}$ acting on an arbitrary system A entangled with a reference system R of the same Hilbert space dimensions, the recovery $\mathcal{R}^{B \rightarrow A}$ of the state of A and R is bounded from below, in the worst case scenario, by the entanglement fidelity of the overall dynamics $(\mathcal{R} \circ \mathcal{N})^{A \rightarrow A}$, namely*

$$\frac{1}{2} \|\mathcal{R} \circ \mathcal{N} - \text{id}\|_{\diamond} \geq 1 - F_e(\mathcal{R} \circ \mathcal{N}). \quad (71)$$

This lower bound holds for both recovery with perfect and incomplete knowledge scenarios in Figs. 1 and 2, respectively. Next, we consider the incomplete knowledge scenario, and analyze the contribution of the spectator system to the lower bound.

2. Contribution of the Spectator System

Consider the scenario described in Fig. 2, which is what we expect for real-time quantum memories. A best estimate $\hat{\theta}$ of the unknown $\theta \in \Theta$ is found by the spectator system for each time-interval over which the value of the *stroboscopic* (slowly varying) variable θ is approximately constant. This characteristic timescale of the stroboscopic noise parameter θ should be larger than the combined characteristic times of the noisy \mathcal{N}_{θ} and the

best-guess recovery $\mathcal{R}_{\hat{\theta}}$ dynamics. Consequently, the relevant total dynamics of the encoded system is given by $\mathcal{R}_{\hat{\theta}} \circ \mathcal{N}_{\theta}$. Applying Corollary 2 to this channel yields

$$\frac{1}{2} \|\mathcal{R}_{\hat{\theta}} \circ \mathcal{N}_{\theta} - id\|_{\diamond} \geq 1 - F_e(\mathcal{R}_{\hat{\theta}} \circ \mathcal{N}_{\theta}). \quad (72)$$

We separate the right hand side into two contributions:

- The first part $1 - F_e(\mathcal{R}_{\theta} \circ \mathcal{N}_{\theta})$ describes the fundamental lower bound on the optimal recovery protocol (see Eq. (71)).
- The second part $F_e(\mathcal{R}_{\theta} \circ \mathcal{N}_{\theta}) - F_e(\mathcal{R}_{\hat{\theta}} \circ \mathcal{N}_{\theta})$ quantifies the contribution of the incomplete knowledge of $\theta \in \Theta$ to the lower bound.

Using Corollary 1, we can set an upper bound to the contribution of the spectator system. By picking $\mathcal{Q}^A \equiv \mathcal{R}_{\theta}^{B \rightarrow A} \circ \mathcal{N}_{\theta}^{A \rightarrow B}$ and $\mathcal{S}^A \equiv \mathcal{R}_{\hat{\theta}}^{B \rightarrow A} \circ \mathcal{N}_{\hat{\theta}}^{A \rightarrow B}$, we arrive at the following information-theoretic characterization to the contribution for the spectator system:

Theorem 2. *The contribution of the incomplete knowledge $\hat{\theta} \approx \theta$ (with $\text{Var}(\hat{\theta}) > 0$) to the entanglement fidelity of recovery of the parameterized noisy channel $\mathcal{N}_{\theta}^{A \rightarrow B}$ is characterized by the diamond distance between the optimum recovery $\mathcal{R}_{\theta}^{A \rightarrow B}$ and the best-guess recovery $\mathcal{R}_{\hat{\theta}}^{A \rightarrow B}$, as follows*

$$F_e(\mathcal{R}_{\theta} \circ \mathcal{N}_{\theta}) - F_e(\mathcal{R}_{\hat{\theta}} \circ \mathcal{N}_{\theta}) \leq \frac{1}{2} \|\mathcal{R}_{\theta} - \mathcal{R}_{\hat{\theta}}\|_{\diamond}. \quad (73)$$

Proof. This follows immediately from

$$\frac{1}{2} \|\mathcal{R}_{\theta} \circ \mathcal{N}_{\theta} - \mathcal{R}_{\hat{\theta}} \circ \mathcal{N}_{\theta}\|_{\diamond} = \frac{1}{2} \|\mathcal{R}_{\theta} - \mathcal{R}_{\hat{\theta}}\|_{\diamond}, \quad (74)$$

and applying Corollary 1 for the optimum recovery $\mathcal{R}_{\theta}^{A \rightarrow B}$ and the best-guess recovery $\mathcal{R}_{\hat{\theta}}^{A \rightarrow B}$ maps. ■

A second information-theoretic characterization exists for the contribution of the lack of knowledge to the lower bound in Eq. (72), in terms of the quantum Fisher information of the spectator dynamics. We frame this as follows:

Theorem 3. *The contribution of the incomplete knowledge $\hat{\theta} \approx \theta$ (with $\text{Var}(\hat{\theta}) > 0$) to the entanglement fidelity of recovery of the parameterized noisy channel $\mathcal{N}_{\theta}^{A \rightarrow B}$ is characterized by the quantum Fisher information of the spectator dynamics \mathcal{M}_{θ} , as follows*

$$\langle F_e(\mathcal{R}_{\theta} \circ \mathcal{N}_{\theta}) - F_e(\mathcal{R}_{\hat{\theta}} \circ \mathcal{N}_{\theta}) \rangle_{p_{\theta}(\hat{\theta}|x)} = g(\theta) \text{Var}(\hat{\theta}), \quad (75)$$

which implies from the QCRB that

$$\langle F_e(\mathcal{R}_{\theta} \circ \mathcal{N}_{\theta}) - F_e(\mathcal{R}_{\hat{\theta}} \circ \mathcal{N}_{\theta}) \rangle_{p_{\theta}(\hat{\theta}|x)} \geq \frac{g(\theta)}{I_{QF}(\mathcal{M}_{\theta})}, \quad (76)$$

where $p_{\theta}(\hat{\theta}|x)$ is the spectator system's probability distribution function (x is the measurement outcome of the

spectator observable $X = \sum_{x \in \mathcal{X}} x \Pi_x$) and $g(\theta)$ is defined as

$$g(\theta) := -\frac{1}{2} \left(\frac{d^2}{d(\delta\theta)^2} F_e(\mathcal{R}_{\theta+\delta\theta} \circ \mathcal{N}_{\theta}) \right) \Big|_{\delta\theta=0}. \quad (77)$$

Proof. The proof follows directly from Taylor expanding the entanglement fidelity with respect to the difference $\delta\theta \equiv \hat{\theta} - \theta$, similar to [58], as follows

$$F_e(\mathcal{R}_{\theta} \circ \mathcal{N}_{\theta}) - F_e(\mathcal{R}_{\hat{\theta}} \circ \mathcal{N}_{\theta}) \quad (78)$$

$$= F_e(\mathcal{R}_{\theta} \circ \mathcal{N}_{\theta}) - F_e(\mathcal{R}_{\theta+\delta\theta} \circ \mathcal{N}_{\theta}) \quad (79)$$

$$\begin{aligned} &= \frac{1}{1!} \left(-\frac{d}{d(\delta\theta)} F_e(\mathcal{R}_{\theta+\delta\theta} \circ \mathcal{N}_{\theta}) \right) \Big|_{\delta\theta=0} \delta\theta \\ &\quad + \frac{1}{2!} \left(-\frac{d^2}{d(\delta\theta)^2} F_e(\mathcal{R}_{\theta+\delta\theta} \circ \mathcal{N}_{\theta}) \right) \Big|_{\delta\theta=0} (\delta\theta)^2 \\ &\quad + \mathcal{O}((\delta\theta)^3). \end{aligned} \quad (80)$$

Taking the expectation of both sides with respect to the spectator system's probability distribution function $p_{\theta}(\hat{\theta}|x)$ yields the main result of the theorem

$$\langle F_e(\mathcal{R}_{\theta} \circ \mathcal{N}_{\theta}) - F_e(\mathcal{R}_{\hat{\theta}} \circ \mathcal{N}_{\theta}) \rangle_{p_{\theta}(\hat{\theta}|x)} = g(\theta) \text{Var}(\hat{\theta}). \quad (81)$$

Note that the expected dependence of the spectator's contribution separates into the product of two functions: the first, $g(\theta)$, depends on the full dynamics of the memory system, and the second, $\text{Var}(\hat{\theta})$, depends on the full dynamics of the spectator system. It turns out that the function $g(\theta)$ could be computed analytically for simple single-qubit channels, such as for the amplitude-damping channel [59].

To summarize, Theorems 2 and 3 characterize the lack of perfect knowledge of the noise parameter θ for any recovery protocol, and hence also the contribution of the spectator system to the fundamental lower bound in Corollary 2.

B. Spectator Dynamics

In the introduction, as well as Figs. 2 and 3, we have emphasised the fact that the spectator system need not be the same physical system as the computational or memory system. Consequently, the dynamics of the spectator system \mathcal{M}_{θ} is generally different from the dynamics $\mathcal{N}_{\theta} = \bigotimes_{i=1}^N \mathcal{N}_{\theta}^{(i)}$ of the N memory qubits, though it still depends on the same environment noise parameter θ . If the spectator system is made out of M subsystems (e.g. qubits), then the independent noise model reads

$$\mathcal{M}_{\theta} = \bigotimes_{i=1}^M \mathcal{M}_{\theta}^{(i)}, \quad (82)$$

where $\mathcal{M}_\theta^{(1)}$ is a quantum channel acting on the i -th subsystem. Note that we assumed negligible spacial variability of the noise parameter θ .

To perform recovery with incomplete knowledge, we need to hypothesise a relation between the spectator and memory qubit dynamics, i.e. $\mathcal{M}_\theta^{(1)}$ and $\mathcal{N}_\theta^{(1)}$. Due to the fact that both types of qubits are subject to the same noisy environment with potentially different coupling strengths, we hypothesise

$$\mathcal{M}_\theta^{(1)} = \mathcal{N}_{f(\theta)}^{(1)}, \quad (83)$$

where $f(\theta) \in [0, 1]$ is a monotone increasing function of its argument. To justify this choice, consider the case where θ has the following form

$$\theta = 1 - e^{-t/T_1}, \quad (84)$$

where T_1 is the spin relaxation time [9, 10]. This is the case e.g. for the qubit amplitude-damping channel, which I consider both in Section V and Section VI. Then, by expressing t/T_1 in terms of θ , we arrive at

$$f_\gamma(\theta) = 1 - (1 - \theta)^\gamma, \quad (85)$$

where $\gamma = T_1^{\text{memo}}/T_1^{\text{spec}}$. The requirement that the spectator qubits should exhibit faster dynamics than the memory qubits translates to $\gamma > 1$.

C. Application to The [4, 1] Code of The Amplitude-Damping Channel

In what follows, we derive the entanglement fidelity $F_e(\mathcal{R}_\theta \circ \mathcal{N}_\theta)$ for the [4, 1] code of the amplitude-damping (AD) channel analytically, following the approach developed in [60], and extending the derivation in [59] to the incomplete knowledge recovery scenario. It is worth noting that analytical approaches to the AD channel have also been taken previously in e.g. [61, 62].

Since the AD channel is covariant with respect to the group $\{I, Z\}$, the Eastin-Knill theorem [63] guarantees that no perfect QEC codes exist. However, approximate codes for the AD channel have been developed in [7] and later on, channel-adapted codes have been developed [6], where the recovery depends on the value of the noise parameter. The developed techniques have also been extended beyond the [4, 1] code and towards more general $[2K+1, K]$ codes [6, 7] (where K logical qubits are encoded into $N = 2K+1$ physical/memory qubits).

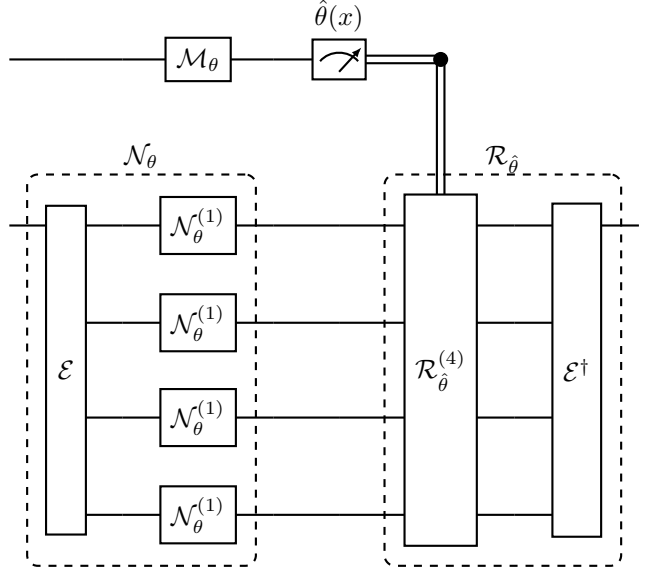


FIG. 3. Spectator-based quantum error correction of the [4, 1] code of the amplitude-damping channel: A single logical qubit is encoded into four physical qubits using the encoding channel $\mathcal{E} : \mathcal{H}_2 \rightarrow \mathcal{H}_2^{\otimes 4}$ in Eqs. (87) and (88), where \mathcal{H}_2 denotes the two dimensional Hilbert space of a single qubit system. Unbiased estimation $\hat{\theta}(x)$ of the noise parameter θ of the amplitude-damping channel is conducted by measuring the spectator observable $X = \sum_{x \in \mathcal{X}} x \Pi_x$, with possible outcomes $x \in \mathcal{X}$ (where Π_x projects onto the subspace of $X = x$). The estimated value $\hat{\theta}(x)$ is fed into the recovery operation described in detail in [6] that is adapted for the amplitude-damping channel.

1. The Amplitude-Damping Channel

The single-qubit AD channel is defined as $\mathcal{N}_\theta^{(1)}(\cdot) = N_0(\cdot)N_0^\dagger + N_1(\cdot)N_1^\dagger$, where

$$N_0 = \begin{pmatrix} 1 & 0 \\ 0 & \sqrt{1-\theta} \end{pmatrix}, \quad N_1 = \begin{pmatrix} 0 & \sqrt{\theta} \\ 0 & 0 \end{pmatrix}. \quad (86)$$

The Kraus operators N_0, N_1 are often called the “no-damping” and “damping” errors, respectively. Here, the noise parameter $\theta(t) = 1 - \exp(-t/T_1)$ depends on time t and the relaxation time T_1 [10, 57]. We follow the usual notation in quantum information, where the dependence of the noisy channel (and hence also the noise parameter) on time is suppressed.

2. The Approximate [4, 1] Code

Assuming an independent noise model, we recall the encoding $\mathcal{E} : \mathcal{D}(\mathcal{H}) \rightarrow \mathcal{D}(\mathcal{C})$ of the [4,1] code [7] from a 1-qubit physical state to a 4-qubit logical state, where

$\mathcal{C} = \text{span}\{|0_L\rangle, |1_L\rangle\} \subset \mathcal{H}^{\otimes 4}$, as follows

$$|0\rangle \rightarrow |0_L\rangle := \frac{1}{\sqrt{2}} (|0000\rangle + |1111\rangle) \quad (87)$$

$$|1\rangle \rightarrow |1_L\rangle := \frac{1}{\sqrt{2}} (|0011\rangle + |0011\rangle), \quad (88)$$

and hence $\mathcal{E}(\cdot) := C(\cdot)C^\dagger$, where $C = |0_L\rangle\langle 0| + |1_L\rangle\langle 1|$. The encoded Pauli operators $\sigma_{\text{enc}} = \mathcal{E}(\sigma)$ for $\sigma \in \{I, X, Y, Z\}$ read

$$I_{\text{enc}} = |0_L\rangle\langle 0_L| + |1_L\rangle\langle 1_L| \quad (89)$$

$$X_{\text{enc}} = |0_L\rangle\langle 1_L| + |1_L\rangle\langle 0_L| \quad (90)$$

$$Y_{\text{enc}} = -i|0_L\rangle\langle 1_L| + i|1_L\rangle\langle 0_L| \quad (91)$$

$$Z_{\text{enc}} = |0_L\rangle\langle 0_L| - |1_L\rangle\langle 1_L|. \quad (92)$$

By definition, the encoded Pauli operators only act on states in the codespace \mathcal{C} . However, in the stabilizer formalism, the logical Pauli operators I_L, X_L, Y_L , and Z_L are defined on the full 4-qubit Hilbert space. For example, the generators of the stabilizer set for the [4, 1] code is given by $S = \{S_j\}_{j=1}^3 = \{XXX, ZZII, IIIZ\}$, along with the logical Pauli operators $X_L = XXII$, $Y_L = YXZI$, and $Z_L = ZIZI$. The link between the encoded and logical Pauli operators is found by restricting the action of the latter to the codespace. Namely, $\sigma_{\text{enc}} = \mathcal{E}(\sigma) = \Pi\sigma_L$, where $\Pi = \sum_{j=1}^3 S_j/|S|$ is the projection onto the codespace \mathcal{C} corresponding to the set of stabilizers [60].

We define the noisy channel \mathcal{N}_θ to be the physical noise experienced by the four physical qubits in the [4,1] code post-encoding, as follows

$$\mathcal{N}_\theta = \left(\mathcal{N}_\theta^{(1)} \otimes \mathcal{N}_\theta^{(1)} \otimes \mathcal{N}_\theta^{(1)} \otimes \mathcal{N}_\theta^{(1)} \right) \circ \mathcal{E}. \quad (93)$$

Furthermore, we define the decoding recovery channel $\mathcal{R}_{\hat{\theta}}$ to be given by

$$\mathcal{R}_{\hat{\theta}} = \mathcal{E}^\dagger \circ \mathcal{R}_{\hat{\theta}}^{(4)}, \quad (94)$$

where $\mathcal{R}_{\hat{\theta}}^{(4)}$ is taken from Table 1 of [6], which is the channel-adapted recovery of the AD channel (see Fig. 4(b) for the performance of this recovery).

3. Entanglement Fidelity

The entanglement fidelity for single-qubit ($K = 1$) $[N, K]$ codes is given by [59]

$$F_e(\mathcal{R}_\theta \circ \mathcal{N}_\theta) = \frac{1}{4} \text{Tr}[G], \quad (95)$$

where the matrix elements $G_{\sigma\sigma'} = \text{Tr} \left[D_{\hat{\theta},\sigma} \mathcal{N}_\theta [\sigma'_L] \right]$, with $D_{\hat{\theta},\sigma} \equiv 2 \sum_i R_{\hat{\theta},\sigma}^{(4)} \sigma_L R_{\hat{\theta},\sigma}^{(4)\dagger}$, describes the effective dynamics of the Bloch coefficients for the encoded single qubit

[60], i.e. if $\rho_i = \frac{1}{2} \sum_\sigma u_\sigma \sigma$ and $\rho_f = \frac{1}{2} \sum_\sigma v_\sigma \sigma$, then $\vec{v} = G\vec{u}$.

In [59], the authors derived an analytical formula for the entanglement fidelity $F_e(\mathcal{R}_\theta \circ \mathcal{N}_\theta)$ as

$$F_e = \frac{1}{4} \left[1 + \sqrt{2} \text{Re}[\alpha] \tau - 8\tau^2 + (\sqrt{2} \text{Re}[\beta] - 8) \tau^3 + \tau^4 \right], \quad (96)$$

where $\tau = 1 - \theta$ and α, β (with $|\alpha|^2 + |\beta|^2 = 1$) are the complex parameters that the recovery channel depends on. The optimum recovery channel $\mathcal{R}_\theta(\alpha, \beta) = \mathcal{R}(\alpha(\theta), \beta(\theta))$ in [6] is the one that maximizes the entanglement fidelity with respect to α, β for the given value of the noise parameter θ .

To find the dependence of α and β on the noise parameter θ for the optimum recovery, we first rewrite Eq. (96) using $\alpha = |\alpha|e^{i\psi}$ and $\beta = |\beta|e^{i\phi} = \sqrt{1 - |\alpha|^2}e^{i\phi}$, which yields

$$\begin{aligned} F_e(|\alpha|, \psi, \phi; \theta) = & \frac{1}{4} + \frac{\sqrt{2}}{4} |\alpha| \tau \cos \psi - 2\tau^2 \\ & + (\sqrt{2(1 - |\alpha|^2)} \cos \phi - 8) \frac{\tau^3}{4} + \frac{\tau^4}{4}. \end{aligned} \quad (97)$$

Then we take the partial derivatives of this function with respect to the independent parameters $|\alpha| \in [0, 1]$ and $\psi, \phi \in [0, 2\pi)$, to arrive at

$$|\alpha_{\text{opt}}(\theta)| = \frac{1}{\sqrt{1 + \tau^4}} \quad \text{and} \quad (\psi_{\text{opt}}, \phi_{\text{opt}}) = \{(0, 0), (\pi, \pi)\}. \quad (98)$$

By simple substitution, we can check that $(\psi, \phi) = (0, 0)$ is the pair that maximizes the entanglement fidelity function, with the value

$$F_e(\mathcal{R}_\theta \circ \mathcal{N}_\theta) = \frac{1}{4} \left[1 + \tau \sqrt{2(1 + \tau^4)} + \tau^2 (8 - 8\tau + \tau^2) \right]. \quad (99)$$

Now let us find an analytical formula for the incomplete knowledge scenario $F_e(\mathcal{R}_{\hat{\theta}} \circ \mathcal{N}_\theta)$. Note that in Eq. (96), the dependence of the recovery $\mathcal{R}_{\hat{\theta}}(\alpha, \beta) = \mathcal{R}(\alpha(\hat{\theta}), \beta(\hat{\theta}))$ on the estimated noise parameter $\hat{\theta}$ enters only through α and β [6]. Therefore, we can use the optimum values $|\alpha_{\text{opt}}(\hat{\theta})| = 1/\sqrt{1 + \tau(\hat{\theta})}$ and $\psi_{\text{opt}} = \phi_{\text{opt}} = 0$ and plug it back into Eq. (96), which yields

$$\begin{aligned} F_e(|\alpha(\hat{\theta})_{\text{opt}}|; \theta) = & \frac{1}{4} + \frac{\sqrt{2}}{4} |\alpha_{\text{opt}}(\hat{\theta})| \tau(\theta) - 2\tau^2(\theta) \\ & + \left(\sqrt{2(1 - |\alpha_{\text{opt}}(\hat{\theta})|^2)} - 8 \right) \frac{\tau(\theta)^3}{4} + \frac{\tau(\theta)^4}{4}. \end{aligned} \quad (100)$$

Further algebraic simplifications yield

$$F_e(|\alpha(\theta)_{\text{opt}}|; \theta) - F_e(|\alpha(\hat{\theta})_{\text{opt}}|; \theta)$$

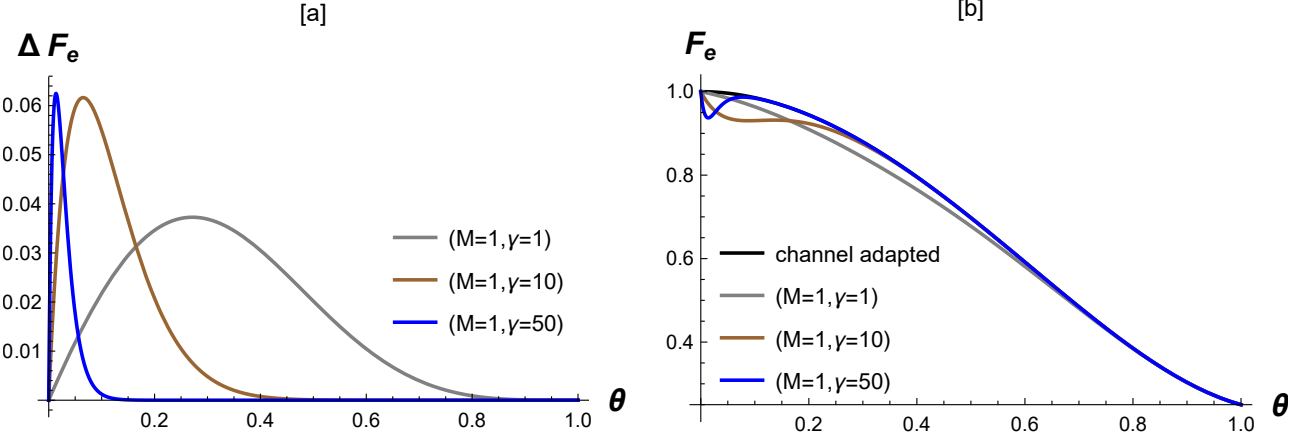


FIG. 4. The spectator system is taken to be a single qubit ($M = 1$) with varying values of the physical parameter γ in Eq. (85). Both subfigures consider the channel-adapted approximate [4, 1] code of the amplitude damping channel [6]. (a) Entanglement fidelity difference between the cases of perfect and incomplete knowledge recovery protocols. (b) Comparison between the entanglement fidelities for perfect [6, 59] and incomplete knowledge recovery protocols. In both figures, we assume the best-case scenario where the spectator system saturates the QCRB during parameter estimation.

$$= \frac{\tau^3(\theta)}{\sqrt{2}(1 + \tau^4(\theta))^{3/2}}(\theta - \hat{\theta})^2 + \mathcal{O}\left((\theta - \hat{\theta})^3\right). \quad (101)$$

Finally, taking the expectation of both sides with respect to the spectator system's probability distribution function $p_\theta(\hat{\theta}|x)$ (where x is the measurement outcome of the spectator observable $X = \sum_{x \in \mathcal{X}} x \Pi_x$) yields

$$\left\langle F_e(|\alpha(\theta)_{\text{opt}}|; \theta) - F_e(|\alpha(\hat{\theta})_{\text{opt}}|; \theta) \right\rangle = h(\theta) \text{Var}(\hat{\theta}), \quad (102)$$

where

$$h(\theta) = \frac{(1 - \theta)^3}{\sqrt{2}(1 + (1 - \theta)^4)^{3/2}}, \quad (103)$$

and we have used the fact that $\hat{\theta}$ is an unbaised estimate of θ . This equality determines the average contribution of the spectator system in the lower bound in Eq. (72) for the [4, 1] AD code. As we can see, since the spectator system is used to conduct parameter estimation, the variance $\text{Var}(\hat{\theta})$ in this estimate is fundamentally bounded by the QCRB determined by the quantum Fisher information, i.e. $\text{Var}(\hat{\theta}) \geq 1/I_{\text{QF}}(\mathcal{M}_\theta)$.

It has been shown that the RLD QFI for the AD channel diverges (see the example discussed in [64] for generalized AD channels), however the SLD QFI is finite and known [65] to be equal to $I_{\text{QF}}(\mathcal{N}_\theta^{(1)}) = 1/(\theta(1 - \theta))$ and

hence

$$I_{\text{QF}}(\mathcal{M}_\theta^{(1)}) = \frac{1}{f_\gamma(\theta)(1 - f_\gamma(\theta))}, \quad (104)$$

where $f_\gamma(\theta)$ is given by Eq. (85) (or more generally, by Eq. (83)). If the spectator system is made out of M qubits, then the QFI scales linearly with M due to the property $I_{\text{QF}}(\mathcal{M}_\theta^{(1) \otimes M}) = M I_{\text{QF}}(\mathcal{M}_\theta^{(1)})$, assuming an independent noise model (see Eq. (82)). However, note that we can only realistically improve the QCRB to a certain degree without dropping the negligible spacial variability assumption of the noise parameter θ [16].

To summarize, the contribution of the spectator system to the entanglement fidelity of the [4, 1] code of the amplitude-damping channel is determined by two parameters: the number of spectator qubits used (M) and their physical nature ($\gamma = T_1^{\text{memo}}/T_1^{\text{spec}}$), as follows

$$\langle \Delta F_e \rangle \geq \frac{h(\theta)}{M f_\gamma(\theta)(1 - f_\gamma(\theta))}, \quad (105)$$

where the functions $h(\theta)$ and $f_\gamma(\theta)$ are given by Eqs. (103) and (85), respectively. When the QCRB is saturated, the resulting entanglement fidelity is illustrated in Fig. 4 for various values of the spectator parameter γ .

VI. RECOVERY BOUNDS IN THE MULTI-CYCLE SCENARIO

A. The Multi-Cycle Case

In the article, I have considered a single-cycle recovery, i.e. when the noisy channel \mathcal{N}_θ is applied only once. However, extensions to the multi-cycle regime are also important for real-time applications. A thorough study of the multi-cycle case is beyond the scope of the current article. However, here I present some useful bounds to stimulate future discussions.

To start, consider a stroboscopically varying noise parameter θ

$$\theta_1 \rightarrow \theta_2 \rightarrow \cdots \rightarrow \theta_n, \quad (106)$$

where n is the number of timesteps $T = n\Delta t$ and Δt is smaller than the characteristic time of the noise parameter θ (i.e. the expected time in which the value of θ will change appreciably). The corresponding set of real-time estimates by the spectator is given by

$$\hat{\theta}_1 \rightarrow \hat{\theta}_2 \rightarrow \cdots \rightarrow \hat{\theta}_n. \quad (107)$$

Next, we would like to introduce a shorthand notation to describe real-time recovery protocols. We denote the distinguishability measure between $\forall \rho \in \mathcal{D}(\mathcal{H})$ and any n -cycle recovery process by

$$\mathbf{D}_{\theta_n \theta_{n-1} \cdots \theta_1}^{\hat{\theta}_n \hat{\theta}_{n-1} \cdots \hat{\theta}_1}(\rho) := \mathbf{D}(\mathcal{I}_{\theta_n \theta_{n-1} \cdots \theta_1}^{\hat{\theta}_n \hat{\theta}_{n-1} \cdots \hat{\theta}_1}(\rho), \rho), \quad (108)$$

where

$$\mathcal{I}_{\theta_n \theta_{n-1} \cdots \theta_1}^{\hat{\theta}_n \hat{\theta}_{n-1} \cdots \hat{\theta}_1} := \mathcal{R}_{\hat{\theta}_n} \circ \mathcal{N}_{\theta_n} \circ \mathcal{R}_{\hat{\theta}_{n-1}} \circ \mathcal{N}_{\theta_{n-1}} \cdots \circ \mathcal{R}_{\hat{\theta}_1} \circ \mathcal{N}_{\theta_1}, \quad (109)$$

is an n -cycle concatenation between the noisy channel (with changing noise parameter values in each timestep) and the corresponding best-guess recovery.

B. Recurrence Inequalities for Composite Average Channel Fidelity

So far, we have found a lower bound on the desired distinguishability measure in terms of the composite channel entanglement fidelity for the single-cycle case, e.g. see Eqs. (71) and (72). To extend to the multi-cycle scenario, one option is to consider the entanglement fidelity of $\mathcal{I}_{\theta_n \theta_{n-1} \cdots \theta_1}^{\hat{\theta}_n \hat{\theta}_{n-1} \cdots \hat{\theta}_1}$. However, a more insightful approach is to express this entanglement fidelity in terms of individual cycle fidelities. Specifically, this is accomplished by the use of the entanglement fidelities of $\mathcal{I}_{\theta_{n-1} \cdots \theta_1}^{\hat{\theta}_{n-1} \cdots \hat{\theta}_1}$ and $\mathcal{I}_{\theta_n}^{\hat{\theta}_n}$. Bounding composite channel fidelities using individual channel fidelities has been studied previously in e.g. [27]. The following lemma is largely taken from [27], using the χ -matrix representation of quantum dynamics

(see Appendix A for a self-contained review).

Lemma 4. ([27]) *Given the χ -matrix elements χ_{00}^Q , χ_{00}^S of the channels \mathcal{Q} , \mathcal{S} , respectively, the composite channel $\mathcal{S} \circ \mathcal{Q}$ χ -matrix element $\chi_{00}^{\mathcal{S} \circ \mathcal{Q}}$ is bounded from above (and hence the corresponding error angle $\delta^{\mathcal{S} \circ \mathcal{Q}}$ is bounded from below), as follows*

$$\frac{\chi_{00}^{\mathcal{S} \circ \mathcal{Q}}}{d} \leq \cos^2 \left(\arccos \sqrt{\frac{\chi_{00}^S}{d}} - \arccos \sqrt{\frac{\chi_{00}^Q}{d}} \right), \quad (110)$$

or more simply

$$\delta^{\mathcal{S} \circ \mathcal{Q}} \geq |\delta^{\mathcal{S}} - \delta^{\mathcal{Q}}|. \quad (111)$$

The inequality is saturated iff $v_{ij} = 1$, $\phi_i^Q = \phi_{i'}^Q$, and $\phi_j^S = \phi_{j'}^S$ for $\forall i, i' = 1, \dots, K(\mathcal{Q})$ and $\forall j, j' = 1, \dots, K(\mathcal{S})$. The quantities v_{ij} , ϕ_i^Q , and ϕ_j^S are defined in Appendix E in terms of the Kraus operators of \mathcal{Q} , \mathcal{S} and the d^2 matrix basis elements of $\mathcal{L}(\mathcal{H})$.

For completeness, the proof of this lemma is found in Appendix E.

Let us denote by $\mathcal{Q} \equiv \mathcal{I}_{\theta_{n-1} \cdots \theta_1}^{\hat{\theta}_{n-1} \cdots \hat{\theta}_1}$ and $\mathcal{S} \equiv \mathcal{I}_{\theta_n}^{\hat{\theta}_n}$, such that $\mathcal{S} \circ \mathcal{Q} = \mathcal{I}_{\theta_n \theta_{n-1} \cdots \theta_1}^{\hat{\theta}_n \hat{\theta}_{n-1} \cdots \hat{\theta}_1}$. We further use the notation $\chi_{00}^{1 \rightarrow n}$, $\chi_{00}^{1 \rightarrow (n-1)}$, χ_{00}^n , $\delta^{1 \rightarrow n}$, $\delta^{1 \rightarrow (n-1)}$, and δ^n to replace $\chi_{00}^{\mathcal{S} \circ \mathcal{Q}}$, $\chi_{00}^{\mathcal{Q}}$, $\chi_{00}^{\mathcal{S}}$, $\delta^{\mathcal{S} \circ \mathcal{Q}}$, $\delta^{\mathcal{Q}}$, and $\delta^{\mathcal{S}}$, respectively. Therefore, we can reframe Lemma 4 by the authors of [27] as the following set of *recurrence inequalities* in the context of spectator-based recovery:

Theorem 4. *Given the entanglement fidelities F_e^i of the single-cycle recovery protocols at each time step $\Delta t = t_{i+1} - t_i$, the n -cycle entanglement fidelity $F_e^{1 \rightarrow n}$ of the multi-cycle recovery protocol is bounded from above by the $(n-1)$ -cycle entanglement fidelity $F_e^{1 \rightarrow (n-1)}$, as*

$$F_e^{1 \rightarrow n} \leq \cos^2 \left(\arccos \sqrt{F_e^{1 \rightarrow (n-1)}} - \arccos \sqrt{F_e^n} \right), \quad (112)$$

or equivalently,

$$\delta^{1 \rightarrow n} \geq |\delta^{1 \rightarrow (n-1)} - \delta^n|. \quad (113)$$

The necessary and sufficient conditions for the saturation of this inequality are identical to that of Lemma 4.

Remark 5. *As noted in [27], the entanglement fidelity of a composite channel exhibits “constructive” and “destructive interference” with respect to the individual channel entanglement fidelities. In our case, we view the n -cycle recovery as a composite channel, where the individual channels are the $(n-1)$ -cycle recovery and the n -th timestep recovery. Therefore, the same phenomenon of constructive and destructive interference applies here. This is purely a multi-cycle recovery phenomenon that is not present in single-cycle recovery case, which has been the main focus of modern literature in QEC.*

C. Contribution of The Spectator System

To identify the contribution of the lack of complete knowledge of θ to the recurrence inequalities, let us consider the error angle

$$\hat{\delta} \equiv \delta^{\mathcal{R}_\theta \circ \mathcal{N}_\theta} := \arccos \sqrt{F_e(\mathcal{R}_\theta \circ \mathcal{N}_\theta)} . \quad (114)$$

We denote by $F_e \equiv F_e(\mathcal{R}_\theta \circ \mathcal{N}_\theta)$, $\hat{F}_e \equiv \hat{F}_e(\mathcal{R}_{\hat{\theta}} \circ \mathcal{N}_\theta)$, and $\Delta F_e \equiv F_e - \hat{F}_e$, and then do the simple manipulation

$$\arccos \sqrt{F_e(\mathcal{R}_{\hat{\theta}} \circ \mathcal{N}_\theta)} = \arccos \sqrt{F_e - \Delta F_e} \quad (115)$$

$$= \arccos \left\{ \sqrt{F_e} \sqrt{1 - \frac{\Delta F_e}{F_e}} \right\} \quad (116)$$

$$\approx \arccos \left\{ \sqrt{F_e} \left[1 - \frac{\Delta F_e}{2F_e} \right] \right\} , \quad (117)$$

and therefore,

$$\cos \hat{\delta} \approx \sqrt{F_e} - \frac{\Delta F_e}{2\sqrt{F_e}} . \quad (118)$$

By denoting $\delta \equiv \arccos \sqrt{F_e}$, we use the trigonometric identity

$$\cos \hat{\delta} - \cos \delta = -2 \sin \frac{\hat{\delta} + \delta}{2} \sin \frac{\hat{\delta} - \delta}{2} , \quad (119)$$

along with the approximations

$$\sin \frac{\hat{\delta} - \delta}{2} \approx \frac{\hat{\delta} - \delta}{2} \quad \text{and} \quad \sin \frac{\hat{\delta} + \delta}{2} \approx \sin \delta = \sqrt{1 - F_e} , \quad (120)$$

to arrive at

$$\hat{\delta} - \delta = \frac{\Delta F_e}{2\sqrt{F_e(1 - F_e)}} \geq 0 . \quad (121)$$

Next, we rewrite Theorem 4 as a recurrence inequality, where the contribution of the spectator system in each time step is clearly separated.

$$F_e^{1 \rightarrow n} \leq \cos^2 \left(\arccos \sqrt{F_e^{1 \rightarrow (n-1)}} - \arccos \sqrt{\hat{F}_e^n} \right) \quad (122)$$

$$\equiv \cos^2 \left(\delta^{1 \rightarrow (n-1)} - \hat{\delta}^n \right) \quad (123)$$

$$= \cos^2 \left(\delta^{1 \rightarrow (n-1)} - \delta^n - (\hat{\delta}^n - \delta^n) \right) . \quad (124)$$

By denoting $a = \delta^{1 \rightarrow (n-1)} - \delta^n$ and $b = \hat{\delta}^n - \delta^n$, and using the trigonometric identities $\cos^2(a - b) = \frac{1}{2} + \frac{1}{2} \cos 2(a - b)$ and $\cos(a - b) = \cos(a) \cos(b) + \sin(a) \sin(b)$, we arrive at

$$\cos^2(a - b) = \frac{1}{2} + \frac{1}{2} (\cos 2a \cos 2b + \sin 2a \sin 2b) \quad (125)$$

$$\approx \cos^2(a) + b \sin(2a) , \quad (126)$$

where we have used the Taylor expansions of the sine and cosine functions to the first order of b . Consequently, we have for Theorem 4 the separation

$$\begin{aligned} F_e^{1 \rightarrow n} &\leq \cos^2 \left(\delta^{1 \rightarrow (n-1)} - \delta^n \right) \\ &+ (\hat{\delta}^n - \delta^n) \sin \left(2(\delta^{1 \rightarrow (n-1)} - \delta^n) \right) , \end{aligned} \quad (127)$$

where the first term is the interference between the previous $n - 1$ cycles and the n -th cycle error angles with perfect knowledge at the n -th step. On the other hand, the second term shows the contribution of the lack of knowledge into the recurrence inequality at the n -th timestep, for a fixed error angle $\delta^{1 \rightarrow (n-1)}$, as

$$\frac{\Delta F_e^n}{2\sqrt{F_e^n(1 - F_e^n)}} \sin \left(2\delta^{1 \rightarrow (n-1)} - 2 \arccos \sqrt{F_e^n} \right) , \quad (128)$$

where we have used Eq. (121). Note that the sign of this contribution depends on difference between the error angles of the previous $n - 1$ cycles and the n -th cycle. Taking the expectation with respect to the probability distribution $p_\theta(\hat{\theta}_n | x_n)$ and using Theorem 3, we arrive at the following:

Theorem 5. *Given the multi-cycle entanglement fidelity $F_e^{1 \rightarrow (n-1)}$ from the previous $n - 1$ cycles, the contribution of the spectator system to the upper bound of the total n -cycle entanglement fidelity $F_e^{1 \rightarrow n}$ is given by*

$$h(\theta_n, F_e^{1 \rightarrow (n-1)}) \text{Var}(\hat{\theta}_n) , \quad (129)$$

where

$$h := \frac{g(\theta_n) \sin(2\delta^{1 \rightarrow (n-1)} - 2 \arccos \sqrt{F_e^n})}{2\sqrt{F_e^n(1 - F_e^n)}} , \quad (130)$$

with

$$g(\theta_n) := -\frac{1}{2} \left(\frac{d^2}{d(\delta\theta_n)^2} F_e(\mathcal{R}_{\theta_n + \delta\theta_n} \circ \mathcal{N}_{\theta_n}) \right) \Big|_{\delta\theta_n=0} . \quad (131)$$

D. Application to [4,1] Code of The Amplitude-Damping Channel

The contribution of the spectator system in multi-cycle bounds can also be computed explicitly for the [4,1] code of the AD channel. For a fixed value of the entanglement fidelity $F_e^{1 \rightarrow (n-1)}$ (or equivalently, $\delta^{1 \rightarrow (n-1)}$) at the $(n-1)$ -th step, we can plot the total upper bound in the case of both complete and incomplete knowledge. The simplest case where the spectator system's parameters are $\gamma = 1$ and $M = 1$ is shown in Fig. 5.

Note that, although we expect the incomplete knowledge about the noise parameter to deteriorate the allowed

values of the entanglement fidelity (as we have shown for single-cycle QEC of the AD channel in Fig. 4(b)), in the multi-cycle scenario, this can play to our advantage due to the coherence between the accumulated error during the prior $(n - 1)$ cycles and the error due to the limited knowledge about the noise parameter at the n -th cycle (see Remark 5). This observation further supports the potential superiority of spectator-based recovery techniques in maintaining real-time quantum memories.

VII. COMPARISON WITH PREVIOUS LITERATURE

A. Relation to Quantum Information-Theoretic Protocols

In the article, we focused on the diamond distance due to its operational meaning in terms of a quantum channel discrimination task. In this context, Corollary 1 could be interpreted as a fundamental bound on the success probability of such a task. A similar bound has already been derived by Pirandola *et al.* in [25] using port-based teleportation [66]. In fact, the bound in [25] is valid for general adaptive protocols.

Furthermore, as current techniques of quantum control have matured, Theorem 4 is not only relevant for multiple recovery rounds, as demonstrated experimentally in e.g. [28]. It can also be applied in various quantum information-theoretic tasks where multiple calls to the noisy channel and adaptive feedback is allowed, such as quantum channel discrimination with adaptive feedback [25, 67, 68].

B. Relation to Robustness of Channel-adapted QEC

Our approach of incomplete knowledge recovery is closely related to the robustness of channel-adapted QEC codes studied previously in literature [53, 54, 69, 70]. To elaborate, since QEC codes are designed to correct the most likely errors, an important question to ask is: how resilient (robust) is the designed QEC code with respect to some arbitrary mixing with the next-most likely errors? The authors of [53] have framed the robustness problem such that it applies both for Pauli and non-Pauli channels, as follows: One first finds the optimum recovery \mathcal{R} of a channel \mathcal{N} (the most likely noise) by maximizing the entanglement fidelity of $\mathcal{R} \circ \mathcal{N}$, and then one mixes the original channel \mathcal{N} with some other channel \mathcal{N}' (the next-most likely noise) by taking their convex combination, i.e. $\mathcal{N}_\mu := (1 - \mu)\mathcal{N} + \mu\mathcal{N}'$ for some mixing parameter $\mu \in [0, 1]$. Then, robustness of the recovery \mathcal{R} with respect to μ is found by considering the entanglement fidelity of $\mathcal{R} \circ \mathcal{N}_\mu$ and observing if it has major variations as a function of the mixing parameter μ . This setup shares some similarities with our approach,

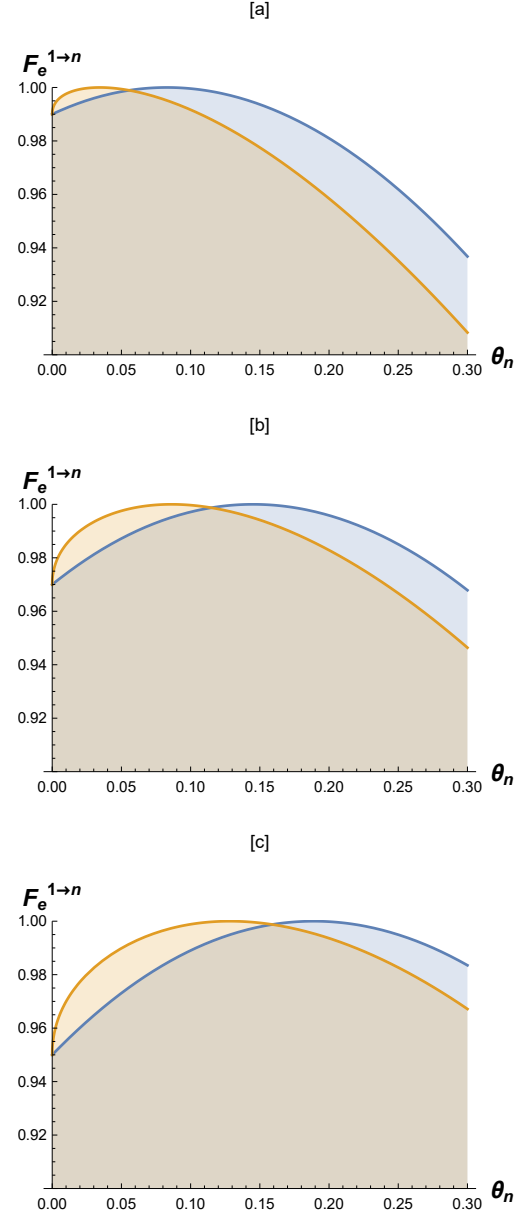


FIG. 5. Subplots show the dependence of $F_e^{1 \rightarrow n}$ on the value of the noise parameter θ_n at the n -th timestep for the [4,1] code of the amplitude-damping channel. The spectator system is taken to have the simplest characteristic parameters ($\gamma = 1, M = 1$). The colored regions indicate allowed values for the entanglement fidelity. The blue color refers to the case of perfect knowledge of θ_n and the orange color to the lack of that knowledge. From top to bottom, the value of the entanglement fidelity in the $(n - 1)$ -th cycle $F_e^{1 \rightarrow (n-1)}$ is picked to be (a) 0.99, (b) 0.97, and (c) 0.95, respectively.

however it has a different quantity of interest, namely the *sensitivity* of entanglement fidelity with respect to changes in the mixing parameter, quantified as the first derivative with respect to μ of

$$F_e(\mathcal{R}_\mu \circ \mathcal{N}_\mu) - F_e(\mathcal{R} \circ \mathcal{N}_\mu), \quad (132)$$

where \mathcal{R}_μ is the optimum recovery of the mixing \mathcal{N}_μ . This is to be contrasted with the quantity of interest in this article (using the parameter notation μ)

$$F_e(\mathcal{R} \circ \mathcal{N}) - F_e(\mathcal{R}_\mu \circ \mathcal{N}). \quad (133)$$

Here, μ plays the role of the uncertainty $\delta\theta \equiv \hat{\theta} - \theta$ in the noise parameter θ , and therefore it has a different interpretation. Namely, there is no next-most likely noise in this description! Instead, μ is the random variable describing the uncertainty in the environment noise parameter and has a finite variance, in accordance with the QCRB.

The possibility of including the channel uncertainty as a probability distribution $p(\mu)$ in the optimization problem of entanglement fidelity has been discussed by Fletcher in [71]. The question then, as mentioned in [53], is: how to pick a physical probability distribution $p(\mu)$? In our picture (spectator-based QEC), this question has a relatively simple answer, as one should always pick the probability distribution that maximizes the Shannon entropy with a fixed expectation and variance (larger or equal to the inverse of the quantum Fisher information). Such a probability distribution is called “the truncated normal distribution”.

C. Relation to [4,1] AD Code Literature

As amplitude-damping (qubit decoherence) is one of the most common noises in quantum systems, developing QEC codes for this particular noise has been a major focus of QEC literature since its inception in 1996. The simplest of such QEC codes is the approximate [4, 1] code [7]. Since then, QEC methods for the AD noise have been developing in sophistication by using various new techniques, such as channel adaptation [6] and semi-definite programming [8]. These techniques have been steadily improving upon the entanglement fidelity of the original [4, 1] code in [7]. However, If we want to implement these techniques for real-time quantum memories (where the decoherence parameter is slowly varying in time), how much of the improvements upon [7] obtained in the last two decades are we likely to retain? The answer to this question, we compare the performance of the [4, 1] code in the incomplete knowledge scenario with previous literature. As spectator systems are characterized by their physical nature $\gamma \geq 1$ and the number of independent subsystems $M \in \mathbb{N}_+$ (see Eq. (82)), the answer will vary from one physical implementation to another. However, we consider the above question in the case $(\gamma = 1, M = 1)$. The results of this comparison are summarized in Fig. 6 and the table below

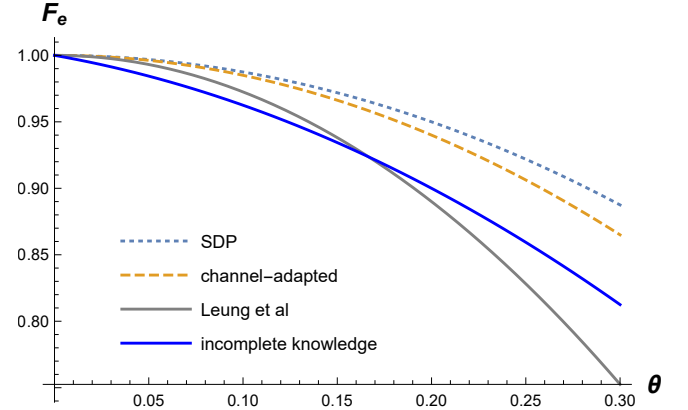


FIG. 6. Comparison with various approaches to the [4, 1] code of the amplitude-damping channel with complete knowledge of the noise parameter θ with spectator parameters ($\gamma = 1, M = 1$). Shown are the performances of the well-known approximate QEC code in Leung *et al.* [7], its channel-adapted version by Fletcher *et al.* [6], its SDP optimized version by Fletcher *et al.* [8], and the incomplete knowledge scenario of the channel-adapted QEC in [6]. Note that improvements upon Leung *et al.* by Fletcher *et al.* [6] are partially lost when incomplete knowledge of θ is available. This is can be thought of as the fundamental fidelity cost of operating a real-time quantum memory. All other (γ, M) spectator-based recoveries lie above the “incomplete knowledge” graph.

Previous literature	F_e to $\mathcal{O}(\theta^3)$ order
Leung <i>et al.</i> [7]	$1 - 2.75\theta^2$
Channel-Adapted [6, 59]	$1 - 1.5\theta^2$
Semi-Definite Programming [8]	$1 - 1.25\theta^2$
Incomplete Knowledge	$1 - 0.25\theta - 1.25\theta^2$

We observe that, due to incomplete knowledge of the noise parameter, the [4, 1] code of the AD channel performs suboptimally to [7] for noise parameter values below a certain threshold $\theta \leq 0.17$. However, beyond that point, the improvements introduced by channel-adapted recoveries and semi-definite programming techniques are preserved, as they still outperform [7], even in the presence of incomplete knowledge about θ . Furthermore, the range of the values of $\theta \in [0, 1]$ for which this outperformance is preserved gets larger the larger we pick γ and/or M (see Fig. 4(a)).

Let us consider one final observation. We noted in Fig. 4 that different value of the spectator parameter γ yield different regions of θ where channel-adapted and semi-definite programming techniques in QEC maintain their improvements upon the approximate [4, 1] code [7], provided that a spectator system is implemented in the incomplete-knowledge recovery protocol. One might observe that, since the value of γ in Eq. (85) generally depend on the couplings of the spectator and memory systems with the environment, the only way to change γ is to change the physical implementation of at least one of these systems. However, recent quantum control

techniques, such as Hamiltonian amplification [72], allow for the tuning of the coupling strengths between an environment and any continuous variable quantum system, with a quadratic coupling Hamiltonian. Therefore, provided that the implementation of either the spectator or memory system has continuous degrees of freedom [73], the Hamiltonian amplification technique yields a practical advantage for spectator-based recovery architectures, as the resulting entanglement fidelities can be manipulated in experiments for any desired region of the noise parameter θ , as seen in Fig. 4(a).

D. Relation to Time-Dependent QEC

In [74], the author suggests that knowledge of the error rates for Pauli channels is not the most useful side-information in QEC. Indeed, as mentioned previously (see Remark 4), the assumption that the optimal recovery channel depends on the environment noise parameter does not hold for Pauli channels whenever perfect QEC is possible (hence the recovery of Pauli channels can be perfectly robust, as shown in [53]). Nevertheless, it is important to note that optimization-based techniques of QEC for Pauli channels do generally benefit from the knowledge of the noise parameter. For example, various types of decoders exist for both repetition codes [75, 76] and surface codes [77], where under the presence of a drifting noise parameter, one can design an adaptive decoder that can track this drift while not interrupting the QEC protocol. In the context of adaptive decoder techniques for repetition and surface codes, this article drives fundamental information-theoretic bounds on their performance, both in the single-cycle and multi-cycle QEC regimes.

VIII. CONCLUSION AND OPEN QUESTIONS

In this article, I considered the problem of building a real-time (drift-adapting) quantum memory and present it as a problem of finding the optimal recovery map for a given noise, with incomplete knowledge of the environment noise parameter (Fig. 2). Using generalized distinguishability measures, I show that fundamental bounds exist for the operation of any quantum memory, regardless of how we decide to quantify its performance (e.g. quantum relative entropy, trace distance, Bures distance, etc.). I compute the lower bound for the diamond distance, showing that it is a linear function of the entanglement fidelity of the full dynamics. To determine the contribution of the incomplete knowledge of the noise parameter to the lower bound, I derive information-theoretic bounds on its performance, first as the diamond distance between the truly optimal and best-guess recovery channels, and second as the quantum Fisher information of the spectator dynamics. This is showcased for the [4, 1] code of the amplitude-damping channel, where channel-

adapted QEC is shown to partially preserve its performance even in the incomplete knowledge scenario, provided that the spectator system architecture is implemented in the quantum memory. Finally, I recall a theorem derived in [27] in the light of upper-bounding multi-cycle recovery by recurrence inequalities, and derive the contribution of the lack of knowledge to the bound. I check this bound for the [4, 1] code of the amplitude-damping channel, observing certain regions of outperformance in the spectator system architecture compared to the perfect knowledge scenario, due to coherence of errors from different cycle numbers as well as the imperfect knowledge error.

The results mentioned above are relevant for various research communities, such as quantum information, quantum control, and quantum computing. To elaborate, the existence of lower bounds on any channel recovery (Theorem 1 and Corollary 1) could be valuable in testing the performance of various optimization-based techniques in QEC to determine if optimal performance is reached. As discussed in Sec. VII, these bounds may also have a broader interest in various domains of quantum information as they hold for any generalized distinguishability measure and between any two quantum channels. Multi-cycle bounds (Theorem 4) might also be useful in adaptive quantum information-theoretic protocols, where many calls to the noisy channel are made. The analysis made for the [4, 1] code of the amplitude-damping channel sheds light on what to expect when implementing such QEC codes in real-time quantum memories [14, 15], while also providing an excited avenue in terms of outperformance in the incomplete knowledge scenario for multi-cycle recovery, which is quickly starting to become a reality [28]. Finally, implementing novel quantum control techniques, such as Hamiltonian amplification for continuous quantum systems [72], might prove useful in controlling the coupling strength of the spectator system. Therefore, one can experimentally optimize over the selection of all possible spectator system parameters without physically changing the spectator system.

There are many open question that follow. For example, although we showcased that the saturation condition of the lower bound in Lemma 1 and Theorem 1 are equivalent to the saturation condition of the joint convexity property of generalized distinguishability measures under certain conditions, determining necessary and sufficient conditions for the latter becomes important for the achievability of the lower bound.

It is interesting to see what the incomplete knowledge scenario might yield for other recovery techniques such as quantum error mitigation [78], dynamical decoupling, and quantum gate teleportation. Furthermore, it might be implemented in continuous (dynamical) recovery using Petz maps [79].

A further open problem is that of implementing the spacial variabilitiy of the noise parameter in the recovery protocol. Various steps have already been made in e.g. [16, 80].

Finally, one would remiss by not considering the large literature on approximate recoverability of quantum states, see e.g. [81–85] and references within. It is interesting to see whether incomplete knowledge recovery protocols would benefit from a similar approach.

IX. ACKNOWLEDGEMENTS

I am grateful to Mark M. Wilde, Hwang Lee, and Stav Haldar for helpful comments and stimulating discussions. I would like to thank Kenneth R. Brown, Mark M. Wilde, and Hwang Lee for the support. I would also like to acknowledge early discussions with Lorenza Viola regarding stroboscopically changing noise parameters, which motivated certain parts of this work. Moreover, I am thankful for the Coates Research Award by the Department of Physics and Astronomy at Louisiana State University. This work was supported by the U.S. Army Research Office through the U.S. MURI Grant No. W911NF-18-1-0218.

[1] Benjamin Schumacher and Michael A Nielsen. Quantum data processing and error correction. *Physical Review A*, 54(4):2629, 1996.

[2] Benjamin Schumacher. Sending entanglement through noisy quantum channels. *Physical Review A*, 54(4):2614, 1996.

[3] Emanuel Knill and Raymond Laflamme. Theory of quantum error-correcting codes. *Physical Review A*, 55(2):900, 1997.

[4] Lorenza Viola and Seth Lloyd. Dynamical suppression of decoherence in two-state quantum systems. *Physical Review A*, 58(4):2733, 1998.

[5] Lorenza Viola, Emanuel Knill, and Seth Lloyd. Dynamical decoupling of open quantum systems. *Physical Review Letters*, 82(12):2417, 1999.

[6] Andrew S Fletcher, Peter W Shor, and Moe Z Win. Channel-adapted quantum error correction for the amplitude damping channel. *IEEE Transactions on Information Theory*, 54(12):5705–5718, 2008.

[7] Debbie W Leung, Michael A Nielsen, Isaac L Chuang, and Yoshihisa Yamamoto. Approximate quantum error correction can lead to better codes. *Physical Review A*, 56(4):2567, 1997.

[8] Andrew S Fletcher, Peter W Shor, and Moe Z Win. Optimum quantum error recovery using semidefinite programming. *Physical Review A*, 75(1):012338, 2007.

[9] Hein-Peter Breuer, Francesco Petruccione, et al. *The theory of open quantum systems*. Oxford University Press on Demand, 2002.

[10] Josu Etxezarreta Martinez, Patricio Fuentes, Pedro Crespo, and Javier Garcia-Frias. Time-varying quantum channel models for superconducting qubits. *npj Quantum Information*, 7(1):1–10, 2021.

[11] Ye Wang, Mark Um, Junhua Zhang, Shuoming An, Ming Lyu, Jing-Ning Zhang, L-M Duan, Dahyun Yum, and Ki-hwan Kim. Single-qubit quantum memory exceeding ten-minute coherence time. *Nature Photonics*, 11(10):646–650, 2017.

[12] Cristian Bonato and Dominic W Berry. Adaptive tracking of a time-varying field with a quantum sensor. *Physical Review A*, 95(5):052348, 2017.

[13] Luis Cortez, Areeya Chantasri, Luis Pedro García-Pintos, Justin Dressel, and Andrew N Jordan. Rapid estimation of drifting parameters in continuously measured quantum systems. *Physical Review A*, 95(1):012314, 2017.

[14] Timothy Proctor, Melissa Revelle, Erik Nielsen, Kenneth Rudinger, Daniel Lobser, Peter Maunz, Robin Blume-Kohout, and Kevin Young. Detecting and tracking drift in quantum information processors. *Nature communications*, 11(1):1–9, 2020.

[15] Swarnadeep Majumder, Leonardo Andreta de Castro, and Kenneth R Brown. Real-time calibration with spectator qubits. *npj Quantum Information*, 6(1):1–9, 2020.

[16] Riddhi Swaroop Gupta, Luke CG Goria, and Michael J Biercuk. Integration of spectator qubits into quantum computer architectures for hardware tune-up and calibration. *Physical Review A*, 102(4):042611, 2020.

[17] Akram Youssry, Gerardo A Paz-Silva, and Christopher Ferrie. Noise detection with spectator qubits and quantum feature engineering. *arXiv preprint arXiv:2103.13018*, 2021.

[18] Emre Togan, Yiwen Chu, Alexei S Trifonov, Liang Jiang, Jeronimo Maze, Lilian Childress, MV Gurudev Dutt, Anders Søndberg Sørensen, Phillip R Hemmer, Alexander S Zibrov, et al. Quantum entanglement between an optical photon and a solid-state spin qubit. *Nature*, 466(7307):730–734, 2010.

[19] D Andrew Golter and Hailin Wang. Optically driven rabi oscillations and adiabatic passage of single electron spins in diamond. *Physical review letters*, 112(11):116403, 2014.

[20] Arshag Danageozian, Ashe Miller, Pratik J Barge, Narayan Bhusal, and Jonathan Patrick Dowling. Noisy coherent population trapping: Applications to noise estimation and qubit state preparation. *Journal of Physics B: Atomic, Molecular and Optical Physics*, 2022.

[21] Shu-Hao Wu, Ethan Turner, and Hailin Wang. Continuous real-time sensing with a nitrogen-vacancy center via coherent population trapping. *Physical Review A*, 103(4):042607, 2021.

[22] Ignas Lekavicius, D Andrew Golter, Thein Oo, and Hailin Wang. Transfer of phase information between microwave and optical fields via an electron spin. *Physical Review Letters*, 119(6):063601, 2017.

[23] Samuel L Braunstein and Carlton M Caves. Statistical distance and the geometry of quantum states. *Physical Review Letters*, 72(22):3439, 1994.

[24] Samuel L Braunstein, Carlton M Caves, and Gerard J Milburn. Generalized uncertainty relations: theory, examples, and lorentz invariance. *annals of physics*, 247(1):135–173, 1996.

[25] Stefano Pirandola, Riccardo Laurenza, Cosmo Lupo, and Jason L Pereira. Fundamental limits to quantum channel discrimination. *npj Quantum Information*, 5(1):1–8, 2019.

[26] Giuliano Benenti and Giuliano Strini. Computing the distance between quantum channels: usefulness of the fano representation. *Journal of Physics B: Atomic, Molecular and Optical Physics*, 43(21):215508, 2010.

[27] Arnaud Carignan-Dugas, Joel J Wallman, and Joseph Emerson. Bounding the average gate fidelity of composite channels using the unitarity. *New Journal of Physics*, 21(5):053016, 2019.

[28] Julia Cramer, Norbert Kalb, M Adriaan Rol, Bas Hensen, Machiel S Blok, Matthew Markham, Daniel J Twitchen, Ronald Hanson, and Tim H Taminiau. Repeated quantum error correction on a continuously encoded qubit by real-time feedback. *Nature communications*, 7(1):1–7, 2016.

[29] Michael Reimpell and Reinhard F Werner. Iterative optimization of quantum error correcting codes. *Physical review letters*, 94(8):080501, 2005.

[30] Michał Horodecki, Paweł Horodecki, and Ryszard Horodecki. General teleportation channel, singlet fraction, and quasidistillation. *Physical Review A*, 60(3):1888, 1999.

[31] Tilo Eggeling and Reinhard F Werner. Separability properties of tripartite states with $u \otimes u \otimes u$ symmetry. *Physical Review A*, 63(4):042111, 2001.

[32] Marcus Silva, Easwar Magesan, David W Kribs, and Joseph Emerson. Scalable protocol for identification of correctable codes. *Physical Review A*, 78(1):012347, 2008.

[33] Easwar Magesan. Gaining information about a quantum channel via twirling. Master’s thesis, University of Waterloo, 2008.

[34] Josu Etxezarreta Martínez, Patricio Fuentes, Pedro M Crespo, and Javier García-Friás. Approximating decoherence processes for the design and simulation of quantum error correction codes on classical computers. *IEEE Access*, 8:172623–172643, 2020.

[35] Joseph Emerson, Marcus Silva, Osama Moussa, Colm Ryan, Martin Laforest, Jonathan Baugh, David G Cory, and Raymond Laflamme. Symmetrized characterization of noisy quantum processes. *Science*, 317(5846):1893–1896, 2007.

[36] Christoph Dankert, Richard Cleve, Joseph Emerson, and Etera Livine. Exact and approximate unitary 2-designs and their application to fidelity estimation. *Physical Review A*, 80(1):012304, 2009.

[37] Adam M Meier. *Randomized benchmarking of clifford operators*. PhD thesis, University of Colorado at Boulder, 2013.

[38] Daniel Gottesman. The heisenberg representation of quantum computers. *arXiv preprint quant-ph/9807006*, 1998.

[39] Michael A Nielsen. A simple formula for the average gate fidelity of a quantum dynamical operation. *Physics Letters A*, 303(4):249–252, 2002.

[40] Christoph Dankert. Efficient simulation of random quantum states and operators. *arXiv preprint quant-ph/0512217*, 2005.

[41] Felix Leditzky, Eneet Kaur, Nilanjana Datta, and Mark M Wilde. Approaches for approximate additivity of the holevo information of quantum channels. *Physical Review A*, 97(1):012332, 2018.

[42] Richard Kueng, David M Long, Andrew C Doherty, and Steven T Flammia. Comparing experiments to the fault-tolerance threshold. *Physical review letters*, 117(17):170502, 2016.

[43] Panos Aliferis. Level reduction and the quantum threshold theorem. *arXiv preprint quant-ph/0703230*, 2007.

[44] Alexei Gilchrist, Nathan K Langford, and Michael A Nielsen. Distance measures to compare real and ideal quantum processes. *Physical Review A*, 71(6):062310, 2005.

[45] Andrea Smirne, Nina Megier, and Bassano Vacchini. Holevo skew divergence for the characterization of information backflow. *arXiv preprint arXiv:2201.07812*, 2022.

[46] Sumeet Khatri and Mark M Wilde. Principles of quantum communication theory: A modern approach. *arXiv preprint arXiv:2011.04672*, 2020.

[47] Previous papers have used the notation $\mathbf{D}(\rho\|\sigma)$, rather than $\mathbf{D}(\rho, \sigma)$, to indicate the generalize distinguishability measure between ρ and σ . Here, we use the latter notation to emphasise the role that \mathbf{D} plays also as a distance measure in deriving standard upper bounds in the context of QEC. Please Appendix D for more details.

[48] Mark M Wilde, Mario Berta, Christoph Hirche, and Eneet Kaur. Amortized channel divergence for asymptotic quantum channel discrimination. *Letters in Mathematical Physics*, 110(8):2277–2336, 2020.

[49] Giulio Chiribella, G Mauro D’Ariano, and Paolo Perinotti. Transforming quantum operations: Quantum supermaps. *EPL (Europhysics Letters)*, 83(3):30004, 2008.

[50] Gilad Gour. Comparison of quantum channels by superchannels. *IEEE Transactions on Information Theory*, 65(9):5880–5904, 2019.

[51] Antonio Acín. Statistical distinguishability between unitary operations. *Physical review letters*, 87(17):177901, 2001.

[52] John Watrous. Semidefinite programs for completely bounded norms. *arXiv preprint arXiv:0901.4709*, 2009.

[53] Gábor Balló and Péter Gurin. Robustness of channel-adapted quantum error correction. *Physical Review A*, 80(1):012326, 2009.

[54] Robert L Kosut, Alireza Shabani, and Daniel A Lidar. Robust quantum error correction via convex optimization. *Physical review letters*, 100(2):020502, 2008.

[55] Robert L Kosut and Daniel A Lidar. Quantum error correction via convex optimization. *Quantum Information Processing*, 8(5):443–459, 2009.

[56] Daniel Gottesman. *Stabilizer codes and quantum error correction*. California Institute of Technology, 1997.

[57] Michael A Nielsen and Isaac Chuang. *Quantum computation and quantum information*, 2002.

[58] Jing Liu, Heng-Na Xiong, Fei Song, and Xiaoguang Wang. Fidelity susceptibility and quantum fisher information for density operators with arbitrary ranks. *Physica A: Statistical Mechanics and its Applications*, 410:167–173, 2014.

[59] Yun Zhan and Xiao-Yu Chen. Entanglement fidelity of channel adaptive quantum codes. *Chinese Physics B*, 22(1):010308, 2013.

[60] Benjamin Rahn, Andrew C Doherty, and Hideo Mabuchi. Exact performance of concatenated quantum codes. *Physical Review A*, 66(3):032304, 2002.

[61] Carlo Cafaro and Peter van Loock. Approximate quantum error correction for generalized amplitude-damping errors. *Physical Review A*, 89(2):022316, 2014.

[62] Carlo Cafaro and Peter van Loock. A simple comparative analysis of exact and approximate quantum error correction. *Open Systems & Information Dynamics*, 21(03):1450002, 2014.

[63] Bryan Eastin and Emanuel Knill. Restrictions on transversal encoded quantum gate sets. *Physical review letters*, 102(11):110502, 2009.

[64] Vishal Katariya and Mark M Wilde. Geometric distinguishability measures limit quantum channel estimation and discrimination. *Quantum Information Processing*, 20(2):1–170, 2021.

[65] Akio Fujiwara. Estimation of a generalized amplitude-damping channel. *Physical Review A*, 70(1):012317, 2004.

[66] Satoshi Ishizaka and Tohya Hiroshima. Asymptotic teleportation scheme as a universal programmable quantum processor. *Physical review letters*, 101(24):240501, 2008.

[67] Giulio Chiribella, Giacomo M D’Ariano, and Paolo Perinotti. Memory effects in quantum channel discrimination. *Physical review letters*, 101(18):180501, 2008.

[68] Masahito Hayashi. Discrimination of two channels by adaptive methods and its application to quantum system. *IEEE Transactions on Information Theory*, 55(8):3807–3820, 2009.

[69] Long Huang, Xiaohua Wu, and Tao Zhou. Robustness of the concatenated quantum error-correction protocol against noise for channels affected by fluctuation. *Physical Review A*, 100(4):042321, 2019.

[70] David Layden, Louisa Ruixue Huang, and Paola Cappellaro. Robustness-optimized quantum error correction. *Quantum Science and Technology*, 5(2):025008, 2020.

[71] Andrew S Fletcher. Channel-adapted quantum error correction. *arXiv preprint arXiv:0706.3400*, 2007.

[72] Christian Arenz, Denys I Bondar, Daniel Burgarth, Cecilia Cormick, and Herschel Rabitz. Amplification of quadratic hamiltonians. *Quantum*, 4:271, 2020.

[73] Daniel Gottesman, Alexei Kitaev, and John Preskill. Encoding a qubit in an oscillator. *Physical Review A*, 64(1):012310, 2001.

[74] Yuchiro Fujiwara. Instantaneous quantum channel estimation during quantum information processing. *arXiv preprint arXiv:1405.6267*, 2014.

[75] Stephen T Spitz, Brian Tarasinski, Carlo WJ Beenakker, and Thomas E O’Brien. Adaptive weight estimator for quantum error correction in a time-dependent environment. *Advanced Quantum Technologies*, 1(1):1800012, 2018.

[76] J Kelly, R Barends, AG Fowler, A Megrant, E Jeffrey, TC White, D Sank, JY Mutus, B Campbell, Yu Chen, et al. Scalable in situ qubit calibration during repetitive error detection. *Physical Review A*, 94(3):032321, 2016.

[77] Ming-Xia Huo and Ying Li. Learning time-dependent noise to reduce logical errors: real time error rate estimation in quantum error correction. *New Journal of Physics*, 19(12):123032, 2017.

[78] Ningping Cao, Junan Lin, David Kribs, Yiu-Tung Poon, Bei Zeng, and Raymond Laflamme. Nisq: Error correction, mitigation, and noise simulation. *arXiv preprint arXiv:2111.02345*, 2021.

[79] Hyukjoon Kwon, Rick Mukherjee, and MS Kim. Reversing lindblad dynamics via continuous petz recovery map. *Physical Review Letters*, 128(2):020403, 2022.

[80] Rochus Klesse and Sandra Frank. Quantum error correction in spatially correlated quantum noise. *Physical review letters*, 95(23):230503, 2005.

[81] Ke Li and Andreas Winter. Squashed entanglement, k-extendibility, quantum markov chains, and recovery maps. *Foundations of Physics*, 48(8):910–924, 2018.

[82] Mark M Wilde. Recoverability in quantum information theory. *Proceedings of the Royal Society A: Mathematical, Physical and Engineering Sciences*, 471(2182):20150338, 2015.

[83] Marius Junge, Renato Renner, David Sutter, Mark M Wilde, and Andreas Winter. Universal recovery maps and approximate sufficiency of quantum relative entropy. In *Annales Henri Poincaré*, volume 19, pages 2955–2978. Springer, 2018.

[84] Omar Fawzi and Renato Renner. Quantum conditional mutual information and approximate markov chains. *Communications in Mathematical Physics*, 340(2):575–611, 2015.

[85] Francesco Buscemi, Siddhartha Das, and Mark M Wilde. Approximate reversibility in the context of entropy gain, information gain, and complete positivity. *Physical Review A*, 93(6):062314, 2016.

[86] Isaac L Chuang and Michael A Nielsen. Prescription for experimental determination of the dynamics of a quantum black box. *Journal of Modern Optics*, 44(11–12):2455–2467, 1997.

[87] Masoud Mohseni, Ali T Rezakhani, and Daniel A Lidar. Quantum-process tomography: Resource analysis of different strategies. *Physical Review A*, 77(3):032322, 2008.

[88] Emanuel Knill, Dietrich Leibfried, Rolf Reichle, Joe Britton, R Brad Blakestad, John D Jost, Chris Langer, Roee Ozeri, Signe Seidelin, and David J Wineland. Randomized benchmarking of quantum gates. *Physical Review A*, 77(1):012307, 2008.

[89] Joshua Combes, Christopher Ferrie, Chris Cesare, Markus Tiersch, Gerard J Milburn, Hans J Briegel, and Carlton M Caves. In-situ characterization of quantum devices with error correction. *arXiv preprint arXiv:1405.5656*, 2014.

[90] Shelby Kimmel, Marcus P da Silva, Colm A Ryan, Blake R Johnson, and Thomas Ohki. Robust extraction of tomographic information via randomized benchmarking. *Physical Review X*, 4(1):011050, 2014.

[91] David Gross, Koenraad Audenaert, and Jens Eisert. Evenly distributed unitaries: On the structure of unitary designs. *Journal of mathematical physics*, 48(5):052104, 2007.

Appendix A: χ -Matrix Representation of Quantum Channels

Besides the well-known Kraus and Stienspring representations of a CPTP map, a lesser-known representation, called the χ -matrix representation [86], is also useful in practice. This is most commonly used in quantum state tomography [57] and is extended to quantum process tomography [87] where state tomography of the

Choi state of a quantum channel is conducted. This is to be contrasted with other approaches in measuring noise, such as randomized benchmarking [88] and QEC itself [89]. Interestingly, the χ -matrix representation can be well motivated in the context of QEC by noting that we can rewrite the “error operators” $\{Q_i\}$ of any noisy map $\mathcal{Q}(\cdot) = \sum_i Q_i(\cdot) Q_i^\dagger$ in terms of a pre-selected “error basis” $\{B_k\}_{k=0}^{d^2-1}$ in $\mathcal{L}(\mathcal{H})$, where $d \equiv \dim \mathcal{H}$. It is particularly useful to pick one of the basis elements, e.g. B_0 , as the “desirable” error (such as being proportional to the unit matrix). Consequently, the coefficient associated with this error component indicates how likely it is that the given Kraus operators of the noisy map will change the state of our quantum system in a “desirable way”. An additional benefit of the χ -matrix representation is that the effects of channel twirling is especially clear [33], as “diagonalization” with respect to the generalized Pauli group. Therefore, the rest of the appendix is devoted to recalling the χ -matrix representation in a self-contained way.

Recall that every CP map $\mathcal{Q}^{A \rightarrow B}$ admits a Kraus decomposition

$$\mathcal{Q}(\cdot) = \sum_{i=1}^K Q_i(\cdot) Q_i^\dagger. \quad (\text{A1})$$

in terms of Kraus operators $\{Q_i\}_{i=1}^K$ satisfying $\sum_{i=1}^K Q_i^\dagger Q_i \leq I_A$, where the equality holds for TP maps. Let us consider a CP map $\mathcal{Q}^{A \rightarrow A} \equiv \mathcal{Q}$, where by denoting $d \equiv \dim(\mathcal{H}^A)$, we can decompose each of the Kraus operators $\{Q_i\}_{i=1}^K$ as a linear combination of some orthonormal operator basis $\{B_k\}_{k=0}^{d^2-1}$ in $\mathcal{L}(\mathcal{H}^A)$, as follows

$$Q_i = \sum_{k=0}^{d^2-1} \langle B_k, Q_i \rangle B_k, \quad (\text{A2})$$

where $\langle B_k, B_l \rangle = \delta_{kl}$, and $\langle \cdot \rangle$ being the Hilbert-Schmidt inner product in $\mathcal{L}(\mathcal{H}^A)$. One could take $B_k \equiv B_{(m,n)} = |m\rangle\langle n|$ for $m, n = \{1, \dots, d\}$, which is known as the standard basis in $\mathcal{L}(\mathcal{H}^A)$. Substituting Eq. (A2) in the Kraus representation of \mathcal{Q} , we get

$$\mathcal{Q}(\cdot) = \sum_{k=0}^{d^2-1} \sum_{l=0}^{d^2-1} \chi_{kl}^{\mathcal{Q}} B_k(\cdot) B_l^\dagger, \quad (\text{A3})$$

where

$$\chi_{kl}^{\mathcal{Q}} := \sum_{i=1}^K \langle B_k, Q_i \rangle \langle Q_i, B_l \rangle, \quad (\text{A4})$$

is called the χ matrix of the CP map \mathcal{Q} . It is easy to see that the χ matrix is a positive semi-definite matrix. This matrix has d^4 complex entries, corresponding to the matrix entries of the superoperator \mathcal{Q} in the Liouville

representation (see, e.g. [27, 90]), namely

$$\hat{\mathcal{Q}} := \sum_{k=0}^{d^2-1} \sum_{l=0}^{d^2-1} \chi_{kl}^{\mathcal{Q}} |B_k\rangle \langle B_l|, \quad (\text{A5})$$

where $|B_k\rangle$ is the $d^2 \times 1$ vector corresponding to the $d \times d$ matrix B_k . The number of independent entries of the χ matrix is reduced from d^4 to $d^4 - d^2$ complex numbers if the CP map \mathcal{Q} is also TP, since for each of the d^2 standard basis elements $|n\rangle\langle m|$ in $\mathcal{L}(\mathcal{H}^A)$, the map \mathcal{Q} must also preserve the trace, which leads to d^2 constraints.

In the context of QEC, it is convenient to choose our operator basis in $\mathcal{L}(\mathcal{H}^A)$ such that B_0 indicates a “desirable effect” on a quantum state. Here $B_0 \equiv I/\sqrt{d}$ is desirable for QEC, but for other applications, B_0 could be chosen differently. Next, we write Eq. (A2) for a fixed $i = 1, \dots, K$, as

$$Q_i = \langle B_0, Q_i \rangle B_0 + \sum_{k=1}^{d^2-1} \langle B_k, Q_i \rangle B_k. \quad (\text{A6})$$

Then, by multiplying both sides on the left by Q_i^\dagger and taking the trace, we arrive at

$$\langle Q_i, Q_i \rangle = |\langle B_0, Q_i \rangle|^2 + \sum_{k=1}^{d^2-1} |\langle B_k, Q_i \rangle|^2, \quad (\text{A7})$$

or equivalently,

$$\frac{|\langle B_0, Q_i \rangle|^2}{\langle Q_i, Q_i \rangle} + \sum_{k=1}^{d^2-1} \frac{|\langle B_k, Q_i \rangle|^2}{\langle Q_i, Q_i \rangle} = 1. \quad (\text{A8})$$

By denoting $q_i^2 := \langle Q_i, Q_i \rangle$, $|\cos(\phi_i)| := |\langle B_0, Q_i \rangle|/q_i$, and $v_{i,k} |\sin(\phi_i)| := |\langle B_k, Q_i \rangle|/q_i$ with some real weights $\{v_{i,k}\}_{k=1}^{d^2-1}$ satisfying $\sum_{k=1}^{d^2-1} v_{i,k}^2 = 1$, we can rewrite the previous equation in a simple form

$$\cos^2(\phi_i) + \sin^2(\phi_i) = 1 \text{ for } \forall i = 1, \dots, K, \quad (\text{A9})$$

where the angle ϕ_i indicates how “close” the error Q_i is to the “desirable error” B_0 . Note that, if \mathcal{Q} is also TP, then $\sum_{i=1}^K q_i^2 = \sum_{i=1}^K \langle Q_i, Q_i \rangle = \text{Tr}[I] = d$.

Due to the unitary freedom of choosing the Kraus operators of any fixed quantum channel from its Steinspring dilation [57], the χ matrix is not uniquely determined. Therefore, using the phase freedom $Q_i \rightarrow Q_i e^{i\omega_i}$ (which is a special case of the unitary freedom mentioned above), we can always choose the phases ω_i for $i = 1, \dots, K$ such that all the inner products $\langle B_0, Q_i \rangle$ with the basis element B_0 are all non-negative. This means that we can pick $\phi_i \in [0, \pi/2]$. Finally, the additional phase in $\langle B_k, Q_i \rangle$ can always be placed in the vector v_k , which

leads to the final decomposition

$$Q_i = q_i \left(\cos(\phi_i) B_0 + \sin(\phi_i) \sum_{k=1}^{d^2-1} v_{i,k} B_k \right), \quad (\text{A10})$$

where $\{v_{i,k}\}_{k=1}^{d^2-1}$ are now complex numbers with $\sum_{k=1}^{d^2-1} |v_{i,k}|^2 = 1$. From here, we can easily compute the matrix element $\chi_{00}^{\mathcal{Q}}$, after taking $B_0 = I/\sqrt{d}$, as

$$\chi_{00}^{\mathcal{Q}} = \sum_{i=1}^K q_i^2 \cos^2(\phi_i) = \frac{1}{d} \sum_{i=1}^K |\text{Tr}[Q_i]|^2, \quad (\text{A11})$$

which is consistent with $\chi_{00}^{\mathcal{Q}}/d = F_e(\mathcal{Q}, I/d)$ [1, 2]. Using Eq. (A10) to compute $Q_i^\dagger Q_i$, taking the trace, and using the orthonormality of the operator basis $\{B_k\}_{k=1}^{d^2-1}$, we arrive at

$$\sum_{i=1}^K \langle Q_i, Q_i \rangle = \sum_{i=1}^K q_i^2 \leq d, \quad (\text{A12})$$

where the inequality follows from $\sum_i Q_i^\dagger Q_i \leq I$. Combined with Eq. (A11), this implies that $0 \leq \chi_{00}^{\mathcal{Q}} \leq d$, or equivalently $0 \leq F_e(\mathcal{Q}) \leq 1$.

Appendix B: Unitary t -designs

We call a function $P : \mathbb{U}(d) \rightarrow \mathbb{C}$ acting on any unitary U in $\mathbb{U}(d)$ to be polynomial of degree t , if its dependence on the $2d^2$ real entries of U is a polynomial of degree at most t in each of its entries. Given a finite set of unitaries $\{U(x)\}_{x \in \mathcal{X}}$ in $\mathbb{U}(d)$, we say that they form a unitary t -design [36, 91] if the uniform Haar average over $\mathbb{U}(d)$ of any polynomial P of degree t is computed using the uniform average over the finite set $\{U(x)\}_{x \in \mathcal{X}}$ only, as follows

$$\int_{\mathbb{U}(d)} dU P(U) = \frac{1}{|\mathcal{X}|} \sum_{x \in \mathcal{X}} P(U(x)). \quad (\text{B1})$$

It has been shown that for unitary 1 and 2-designs, the above averaging condition can be rewritten in a different form. We say that $\{U(x)\}_{x \in \mathcal{X}}$ forms a unitary 1-design in $\mathbb{U}(d)$ if

$$\frac{1}{|\mathcal{X}|} \sum_{x \in \mathcal{X}} U(x) \rho U^\dagger(x) = \pi, \quad (\text{B2})$$

for all $\rho \in \mathcal{D}(\mathcal{H})$, where $\pi = I/d$ is the maximally mixed state. An example of unitary 1-designs are given by the Pauli group. Further, we say $\{U(x)\}_{x \in \mathcal{X}}$ forms a unitary 2-design in $\mathbb{U}(d)$ if we have the following conditions for

twirling of states or channels [36, 40]

$$\begin{aligned} \int_{\mathbb{U}(d)} dU (U \otimes U) \rho (U \otimes U)^\dagger \\ = \frac{1}{|\mathcal{X}|} \sum_{x \in \mathcal{X}} (U(x) \otimes U(x)) \rho (U(x) \otimes U(x))^\dagger, \end{aligned} \quad (\text{B3})$$

for all $\rho \in \mathcal{D}(\mathcal{H} \otimes \mathcal{H})$, or equivalently

$$\begin{aligned} \int_{\mathbb{U}(d)} dU U^\dagger \mathcal{Q}(U \rho U^\dagger) U \\ = \frac{1}{|\mathcal{X}|} \sum_{x \in \mathcal{X}} U^\dagger(x) \mathcal{Q}(U(x) \rho U^\dagger(x)) U(x), \end{aligned} \quad (\text{B4})$$

for all $\rho \in \mathcal{D}(\mathcal{H})$ and quantum channels \mathcal{Q} . An example of unitary 2-designs are given by the Clifford group [35, 40].

Remark 6. Note that, if $\{U(x)\}_{x \in \mathcal{X}}$ is a unitary t -design, then it also holds that $\{U(x)\}_{x \in \mathcal{X}}$ is a unitary $(t-1)$ -design. For example, the Clifford group forms a unitary 3-design, and hence also a unitary 2-design.

Appendix C: Comment on The Chaining Property

In quantum computing literature, one encounters the chaining property for distance measures [42], which is useful for computing upper bounds on error propagation in fault-tolerant quantum computing. This property is framed as follows: Assume we want to apply two maps \mathcal{Q} and \mathcal{S} in series, however, we only have access to their noisy versions, which we denote by \mathcal{Q}' and \mathcal{S}' , respectively. If the generalized distance measure \mathbf{D} also satisfies the DPI (i.e. \mathbf{D} is also a distinguishability measure), then the chaining property reads

$$\begin{aligned} \mathbf{D}(\mathcal{S} \circ \mathcal{Q}(\rho), \mathcal{S}' \circ \mathcal{Q}'(\rho)) \leq \mathbf{D}(\mathcal{Q}(\rho), \mathcal{Q}'(\rho)) \\ + \mathbf{D}(\mathcal{S}(\rho), \mathcal{S}'(\rho)), \end{aligned} \quad (\text{C1})$$

for all $\rho \in \mathcal{D}(\mathcal{H})$. This is interpreted by saying that the error due to a consecutive application of two faulty channels is no larger than the sum of the errors of applying each of the faulty channels separately. The proof follows by first applying the triangle inequality to the left hand side of the above inequality, followed up by the data-processing inequality. Therefore, the desirable chaining property is derivative from other, more fundamental, properties of \mathbf{D} .

Appendix D: Upper-Bounding Generalized Distance Measures for State Recovery

Here we present upper bounds on generalized distance and distinguishability measures, showing how they get modified when limited knowledge about the noise pa-

parameter $\theta \in \Theta$ is available, both for the single-cycle and multi-cycle cases. Similar to the chaining property, derivation of upper bounds on generalized distance and distinguishability measures is important for analysis of error propagation in noisy quantum processes.

1. Single-Cycle Case

Consider the distance measure \mathbf{D} and assume that for $\forall \rho \in \mathcal{D}(\mathcal{C}) \subseteq \mathcal{D}(\mathcal{H})$, approximate recovery from the noise \mathcal{N}_θ is possible in the presence of perfect information about θ , i.e. $\exists \mathcal{R}_\theta$ such that

$$\mathbf{D}(\mathcal{I}_\theta^\theta(\rho), \rho) \leq \epsilon_\theta \text{ where } \mathcal{I}_\alpha^\beta \equiv \mathcal{R}_\beta \circ \mathcal{N}_\alpha. \quad (\text{D1})$$

Now consider the distance measure $\mathbf{D}(\mathcal{I}_\theta^{\hat{\theta}}(\rho), \rho)$, where $\hat{\theta}$ is the best unbiased estimate of $\theta \in \Theta$. Our goal is to bound this quantity from above by two terms: the first depends on how well we can bound the same distance measure when given perfect knowledge about θ (see Eq. (D1)), and the second should measure our lack of knowledge of the noise parameter θ . This intuition is validated by applying the triangle inequality, as follows

$$\mathbf{D}(\mathcal{I}_\theta^{\hat{\theta}}(\rho), \rho) \leq \mathbf{D}(\mathcal{I}_\theta^{\hat{\theta}}(\rho), \mathcal{I}_\theta^{\hat{\theta}}(\rho)) + \mathbf{D}(\mathcal{I}_\theta^{\hat{\theta}}(\rho), \rho) \quad (\text{D2})$$

$$\leq \mathbf{D}(\mathcal{N}_\theta(\rho), \mathcal{N}_{\hat{\theta}}(\rho)) + \mathbf{D}(\mathcal{I}_\theta^{\hat{\theta}}(\rho), \rho) \quad (\text{D3})$$

$$\leq \mathbf{D}(\mathcal{N}_\theta, \mathcal{N}_{\hat{\theta}}) + \mathbf{D}(\mathcal{I}_\theta^{\hat{\theta}}(\rho), \rho) \quad (\text{D4})$$

$$\leq \mathbf{D}(\mathcal{N}_\theta, \mathcal{N}_{\hat{\theta}}) + \epsilon_{\hat{\theta}} \equiv \epsilon_{\theta, \hat{\theta}}, \quad (\text{D5})$$

where the second inequality follows from the DPI of \mathbf{D} , the third follows from the definition of the generalized distance for channels, and the fourth from the assumption of Eq. (D1). It is worth noting that one can derive a similar upper bound using the recoveries, rather than the noisy channels. The advantage of this approach is that we do not need to assume that \mathbf{D} satisfies the DPI, i.e. it suffices for \mathbf{D} to be a distance measure. To see how, we simply apply the triangle inequality

$$\mathbf{D}(\mathcal{I}_\theta^{\hat{\theta}}(\rho), \rho) \leq \mathbf{D}(\mathcal{I}_\theta^{\hat{\theta}}(\rho), \mathcal{I}_\theta^\theta(\rho)) + \mathbf{D}(\mathcal{I}_\theta^\theta(\rho), \rho) \quad (\text{D6})$$

$$\leq \mathbf{D}(\mathcal{R}_\theta, \mathcal{R}_{\hat{\theta}}) + \epsilon_\theta \equiv \epsilon'_{\theta, \hat{\theta}}, \quad (\text{D7})$$

where we have used the definition of distance measure between channels for the second inequality, as well as Eq. (D1). We will shortly show that DPI becomes necessary when considering the multi-cycle case.

2. Multi-Cycle Case

Let us now extend the upper bound previously derived in the single-cycle case to adaptive multi-cycle recovery. Using the shorthand notation

$$\mathbf{D}_{\alpha_n \alpha_{n-1} \cdots \alpha_1}^{\beta_n \beta_{n-1} \cdots \beta_1}(\rho) \equiv \mathbf{D}(\mathcal{I}_{\alpha_n \alpha_{n-1} \cdots \alpha_1}^{\beta_n \beta_{n-1} \cdots \beta_1}(\rho), \rho), \quad (\text{D8})$$

where

$$\mathcal{I}_{\alpha_n \alpha_{n-1} \cdots \alpha_1}^{\beta_n \beta_{n-1} \cdots \beta_1} \equiv \mathcal{R}_{\beta_n} \circ \mathcal{E}_{\alpha_n} \circ \mathcal{R}_{\beta_{n-1}} \circ \mathcal{E}_{\alpha_{n-1}} \cdots \circ \mathcal{R}_{\beta_1} \circ \mathcal{E}_{\alpha_1}, \quad (\text{D9})$$

and applying the triangle inequality, we get

$$\begin{aligned} \mathbf{D}_{\theta_n \theta_{n-1} \cdots \theta_1}^{\hat{\theta}_n \hat{\theta}_{n-1} \cdots \hat{\theta}_1}(\rho) &\leq \mathbf{D}(\mathcal{I}_{\theta_n \theta_{n-1} \cdots \theta_1}^{\hat{\theta}_n \hat{\theta}_{n-1} \cdots \hat{\theta}_1}(\rho), \mathcal{I}_{\hat{\theta}_n \hat{\theta}_{n-1} \cdots \hat{\theta}_1}^{\hat{\theta}_n \hat{\theta}_{n-1} \cdots \hat{\theta}_1}(\rho)) \\ &\quad + \mathbf{D}_{\hat{\theta}_n \hat{\theta}_{n-1} \cdots \hat{\theta}_1}^{\hat{\theta}_n \hat{\theta}_{n-1} \cdots \hat{\theta}_1}(\rho). \end{aligned} \quad (\text{D10})$$

The second term could be bounded from above by the individual errors $\{\epsilon_{\hat{\theta}_i}\}_{i=1}^n$, using only the triangle inequality, as follows

$$\begin{aligned} \mathbf{D}_{\hat{\theta}_n \hat{\theta}_{n-1} \cdots \hat{\theta}_1}^{\hat{\theta}_n \hat{\theta}_{n-1} \cdots \hat{\theta}_1}(\rho) &\leq \mathbf{D}(\mathcal{I}_{\hat{\theta}_n \hat{\theta}_{n-1} \cdots \hat{\theta}_1}^{\hat{\theta}_n \hat{\theta}_{n-1} \cdots \hat{\theta}_1}(\rho), \mathcal{I}_{\hat{\theta}_{n-1} \cdots \hat{\theta}_1}^{\hat{\theta}_{n-1} \cdots \hat{\theta}_1}(\rho)) \\ &\quad + \mathbf{D}_{\hat{\theta}_{n-1} \cdots \hat{\theta}_1}^{\hat{\theta}_{n-1} \cdots \hat{\theta}_1}(\rho). \end{aligned} \quad (\text{D11})$$

We assume that

$$\mathcal{I}_{\hat{\theta}_{n-1} \cdots \hat{\theta}_1}^{\hat{\theta}_{n-1} \cdots \hat{\theta}_1}(\rho) \in \mathcal{D}(\mathcal{C}), \quad (\text{D12})$$

so that the n -th step approximate recovery with perfect knowledge of θ would be possible, in principle. This leads to

$$\mathbf{D}(\mathcal{I}_{\hat{\theta}_n \hat{\theta}_{n-1} \cdots \hat{\theta}_1}^{\hat{\theta}_n \hat{\theta}_{n-1} \cdots \hat{\theta}_1}(\rho), \mathcal{I}_{\hat{\theta}_{n-1} \cdots \hat{\theta}_1}^{\hat{\theta}_{n-1} \cdots \hat{\theta}_1}(\rho)) \quad (\text{D13})$$

$$= \mathbf{D}(\mathcal{I}_{\hat{\theta}_n}^{\hat{\theta}_n}(\mathcal{I}_{\hat{\theta}_{n-1} \cdots \hat{\theta}_1}^{\hat{\theta}_{n-1} \cdots \hat{\theta}_1}(\rho)), \mathcal{I}_{\hat{\theta}_{n-1} \cdots \hat{\theta}_1}^{\hat{\theta}_{n-1} \cdots \hat{\theta}_1}(\rho)) \leq \epsilon_{\hat{\theta}_n}. \quad (\text{D14})$$

Substituting this result back into Eq. (D11), we get

$$\mathbf{D}_{\hat{\theta}_n \hat{\theta}_{n-1} \cdots \hat{\theta}_1}^{\hat{\theta}_n \hat{\theta}_{n-1} \cdots \hat{\theta}_1}(\rho) \leq \mathbf{D}_{\hat{\theta}_{n-1} \cdots \hat{\theta}_1}^{\hat{\theta}_{n-1} \cdots \hat{\theta}_1}(\rho) + \epsilon_{\hat{\theta}_n}, \quad (\text{D15})$$

and repeating the above two steps yields

$$\mathbf{D}_{\hat{\theta}_n \hat{\theta}_{n-1} \cdots \hat{\theta}_1}^{\hat{\theta}_n \hat{\theta}_{n-1} \cdots \hat{\theta}_1} \leq \sum_{i=1}^n \epsilon_{\hat{\theta}_i}. \quad (\text{D16})$$

The first term in Eq. (D10) is a new error term due to the real-time (drift-adapting) nature of our setup. This term can be bounded from above using the chaining property and the DPI, as follows

$$\begin{aligned} &\mathbf{D}(\mathcal{I}_{\theta_n \theta_{n-1} \cdots \theta_1}^{\hat{\theta}_n \hat{\theta}_{n-1} \cdots \hat{\theta}_1}(\rho), \mathcal{I}_{\hat{\theta}_n \hat{\theta}_{n-1} \cdots \hat{\theta}_1}^{\hat{\theta}_n \hat{\theta}_{n-1} \cdots \hat{\theta}_1}(\rho)) \\ &= \mathbf{D}(\mathcal{I}_{\theta_n}^{\hat{\theta}_n} \circ \mathcal{I}_{\theta_{n-1} \cdots \theta_1}^{\hat{\theta}_{n-1} \cdots \hat{\theta}_1}(\rho), \mathcal{I}_{\hat{\theta}_n}^{\hat{\theta}_n} \circ \mathcal{I}_{\hat{\theta}_{n-1} \cdots \hat{\theta}_1}^{\hat{\theta}_{n-1} \cdots \hat{\theta}_1}(\rho)) \end{aligned} \quad (\text{D17})$$

$$\begin{aligned} &\leq \mathbf{D}(\mathcal{I}_{\theta_n}^{\hat{\theta}_n}(\rho), \mathcal{I}_{\hat{\theta}_n}^{\hat{\theta}_n}(\rho)) + \mathbf{D}(\mathcal{I}_{\theta_{n-1} \cdots \theta_1}^{\hat{\theta}_{n-1} \cdots \hat{\theta}_1}(\rho), \mathcal{I}_{\hat{\theta}_{n-1} \cdots \hat{\theta}_1}^{\hat{\theta}_{n-1} \cdots \hat{\theta}_1}(\rho)) \\ &\leq \mathbf{D}(\mathcal{N}_{\theta_n}(\rho), \mathcal{N}_{\hat{\theta}_n}(\rho)) + \mathbf{D}(\mathcal{I}_{\theta_{n-1} \cdots \theta_1}^{\hat{\theta}_{n-1} \cdots \hat{\theta}_1}(\rho), \mathcal{I}_{\hat{\theta}_{n-1} \cdots \hat{\theta}_1}^{\hat{\theta}_{n-1} \cdots \hat{\theta}_1}(\rho)) \end{aligned} \quad (\text{D18})$$

$$\begin{aligned} &\leq \mathbf{D}(\mathcal{N}_{\theta_n}(\rho), \mathcal{N}_{\hat{\theta}_n}(\rho)) + \mathbf{D}(\mathcal{I}_{\theta_{n-1} \cdots \theta_1}^{\hat{\theta}_{n-1} \cdots \hat{\theta}_1}(\rho), \mathcal{I}_{\hat{\theta}_{n-1} \cdots \hat{\theta}_1}^{\hat{\theta}_{n-1} \cdots \hat{\theta}_1}(\rho)) \\ &\leq \mathbf{D}(\mathcal{N}_{\theta_n}, \mathcal{N}_{\hat{\theta}_n}) + \mathbf{D}(\mathcal{I}_{\theta_{n-1} \cdots \theta_1}^{\hat{\theta}_{n-1} \cdots \hat{\theta}_1}(\rho), \mathcal{I}_{\hat{\theta}_{n-1} \cdots \hat{\theta}_1}^{\hat{\theta}_{n-1} \cdots \hat{\theta}_1}(\rho)). \end{aligned} \quad (\text{D19})$$

$$\begin{aligned} &\leq \mathbf{D}(\mathcal{N}_{\theta_n}, \mathcal{N}_{\hat{\theta}_n}) + \mathbf{D}(\mathcal{I}_{\theta_{n-1} \cdots \theta_1}^{\hat{\theta}_{n-1} \cdots \hat{\theta}_1}(\rho), \mathcal{I}_{\hat{\theta}_{n-1} \cdots \hat{\theta}_1}^{\hat{\theta}_{n-1} \cdots \hat{\theta}_1}(\rho)). \end{aligned} \quad (\text{D20})$$

Repeating the above steps $n - 1$ times, we arrive at the upper bound

$$\mathbf{D}(\mathcal{I}_{\theta_n \theta_{n-1} \cdots \theta_1}^{\hat{\theta}_n \hat{\theta}_{n-1} \cdots \hat{\theta}_1}(\rho), \mathcal{I}_{\hat{\theta}_n \hat{\theta}_{n-1} \cdots \hat{\theta}_1}^{\hat{\theta}_n \hat{\theta}_{n-1} \cdots \hat{\theta}_1}(\rho)) \leq \sum_{i=1}^n \mathbf{D}(\mathcal{N}_{\theta_i}, \mathcal{N}_{\hat{\theta}_i}) . \quad (\text{D21})$$

Combining Eqs. (D16) and (D21) with Eq. (D10), we get

$$D_{\theta_n \theta_{n-1} \cdots \theta_1}^{\hat{\theta}_n \hat{\theta}_{n-1} \cdots \hat{\theta}_1} \leq \sum_{i=1}^n [\mathbf{D}(\mathcal{N}_{\theta_i}, \mathcal{N}_{\hat{\theta}_i}) + \epsilon_{\hat{\theta}_i}] \equiv \sum_{i=1}^n \epsilon_{\theta_i, \hat{\theta}_i} , \quad (\text{D22})$$

which generalizes Eq. (D5) for real-time approximate recovery. This result says that, if AQEC is possible in principle (see Eq. (D12)) when perfect knowledge of θ is available, then AQEC is also possible when knowledge about θ is limited. As we have shown, this holds for both the single cycle and multi-cycle regimes.

Alternatively, we can derive an upper bound that is a function of the recoveries, rather than the noisy channels. This is accomplished as follows

$$\begin{aligned} \mathbf{D}_{\theta_n \theta_{n-1} \cdots \theta_1}^{\hat{\theta}_n \hat{\theta}_{n-1} \cdots \hat{\theta}_1}(\rho) &\leq \mathbf{D}(\mathcal{I}_{\theta_n \theta_{n-1} \cdots \theta_1}^{\hat{\theta}_n \hat{\theta}_{n-1} \cdots \hat{\theta}_1}(\rho), \mathcal{I}_{\theta_n \theta_{n-1} \cdots \theta_1}^{\theta_n \theta_{n-1} \cdots \theta_1}(\rho)) \\ &\quad + \mathbf{D}_{\theta_n \theta_{n-1} \cdots \theta_1}^{\theta_n \theta_{n-1} \cdots \theta_1}(\rho) , \end{aligned} \quad (\text{D23})$$

where the second term is similarly bounded from above by $\sum_{i=1}^n \epsilon_{\theta_i}$, based only on the triangle inequality (see Eq. (D16)). We now upper bound the first term in the above inequality as

$$\begin{aligned} &\mathbf{D}(\mathcal{I}_{\theta_n \theta_{n-1} \cdots \theta_1}^{\hat{\theta}_n \hat{\theta}_{n-1} \cdots \hat{\theta}_1}(\rho), \mathcal{I}_{\theta_n \theta_{n-1} \cdots \theta_1}^{\theta_n \theta_{n-1} \cdots \theta_1}(\rho)) \\ &\leq \mathbf{D}(\mathcal{I}_{\theta_n \theta_{n-1} \cdots \theta_1}^{\hat{\theta}_n \hat{\theta}_{n-1} \cdots \hat{\theta}_1}(\rho), \mathcal{I}_{\theta_n \theta_{n-1} \cdots \theta_1}^{\hat{\theta}_n \theta_{n-1} \cdots \theta_1}(\rho)) \\ &\quad + \mathbf{D}(\mathcal{I}_{\theta_n \theta_{n-1} \cdots \theta_1}^{\hat{\theta}_n \theta_{n-1} \cdots \theta_1}(\rho), \mathcal{I}_{\theta_n \theta_{n-1} \cdots \theta_1}^{\theta_n \theta_{n-1} \cdots \theta_1}(\rho)) \end{aligned} \quad (\text{D24})$$

$$\leq \mathbf{D}(\mathcal{I}_{\theta_{n-1} \cdots \theta_1}^{\hat{\theta}_{n-1} \cdots \hat{\theta}_1}(\rho), \mathcal{I}_{\theta_{n-1} \cdots \theta_1}^{\theta_{n-1} \cdots \theta_1}(\rho)) + \mathbf{D}(\mathcal{R}_{\hat{\theta}_n}, \mathcal{R}_{\theta_n}) , \quad (\text{D25})$$

where we have used the triangle inequality for the first inequality and the DPI and the definition of generalized distance measure between channels for the second inequality. By repeating these two steps $n - 1$ times, we arrive at

$$\mathbf{D}(\mathcal{I}_{\theta_n \theta_{n-1} \cdots \theta_1}^{\hat{\theta}_n \hat{\theta}_{n-1} \cdots \hat{\theta}_1}(\rho), \mathcal{I}_{\theta_n \theta_{n-1} \cdots \theta_1}^{\theta_n \theta_{n-1} \cdots \theta_1}(\rho)) \leq \sum_{i=1}^n \mathbf{D}(\mathcal{R}_{\hat{\theta}_i}, \mathcal{R}_{\theta_i}) . \quad (\text{D26})$$

Consequently, Eq. (D23) yields

$$D_{\theta_n \theta_{n-1} \cdots \theta_1}^{\hat{\theta}_n \hat{\theta}_{n-1} \cdots \hat{\theta}_1} \leq \sum_{i=1}^n [\mathbf{D}(\mathcal{R}_{\theta_i}, \mathcal{R}_{\hat{\theta}_i}) + \epsilon_{\theta_i}] \equiv \sum_{i=1}^n \epsilon_{\theta_i, \hat{\theta}_i} . \quad (\text{D27})$$

Appendix E: Proof of Lemma 4

Here we derive an upper bound on the matrix element $\chi_{00}^{\mathcal{S} \circ \mathcal{Q}}$ of the composite channel $\mathcal{S} \circ \mathcal{Q}$, given the corresponding χ matrix elements $\chi_{00}^{\mathcal{Q}}$ and $\chi_{00}^{\mathcal{S}}$ of the individual channels \mathcal{Q} and \mathcal{S} , respectively. The technique used for the following derivation is based on [27].

Given the Kraus operators $\{Q_i\}_{i=1}^{K(\mathcal{Q})}$, $\{S_j\}_{j=1}^{K(\mathcal{S})}$ of the individual channels \mathcal{Q} and \mathcal{S} , the Kraus operators of the composite channel $\mathcal{S} \circ \mathcal{Q}$ are given by $\{S_j Q_i\}_{i,j}$ for $i = 1, \dots, K(\mathcal{Q})$ and $j = 1, \dots, K(\mathcal{S})$. Therefore, by using Eq. (A10) for the individual Kraus operators and using the notation $\langle Q_i, Q_i \rangle = q_i$ and $\langle S_i, S_i \rangle = s_i$, we find for the Kraus operators of the composite channel

$$\begin{aligned} S_j Q_i &= s_j q_i \cos(\phi_j^{\mathcal{S}}) \cos(\phi_i^{\mathcal{Q}}) B_0^2 \\ &\quad + s_j q_i \sin(\phi_j^{\mathcal{S}}) \cos(\phi_i^{\mathcal{Q}}) \sum_{k=1}^{d^2-1} v_{j,k}^{\mathcal{S}} B_k B_0 \\ &\quad + s_j q_i \cos(\phi_j^{\mathcal{S}}) \sin(\phi_i^{\mathcal{Q}}) \sum_{k=1}^{d^2-1} v_{i,k}^{\mathcal{Q}} B_0 B_k \\ &\quad + s_j q_i \sin(\phi_j^{\mathcal{S}}) \sin(\phi_i^{\mathcal{Q}}) \sum_{k,k'=1}^{d^2-1} v_{j,k}^{\mathcal{S}} v_{i,k'}^{\mathcal{Q}} B_k B_{k'} . \end{aligned} \quad (\text{E1})$$

By substituting into Eq. (A11) and choosing the operator basis elements to be Hermitian (hence $\text{Tr}[B_k B_{k'}] = \langle B_k, B_{k'} \rangle = \delta_{kk'}$, for $k, k' = 0, 1, \dots, n^2 - 1$), we arrive at

$$\begin{aligned} \chi_{00}^{\mathcal{S} \circ \mathcal{Q}} &= \frac{1}{d} \sum_{i,j} s_j^2 q_i^2 |\cos(\phi_j^{\mathcal{S}}) \cos(\phi_i^{\mathcal{Q}})| \\ &\quad + (v_j^{\mathcal{S}} \bullet v_i^{\mathcal{Q}}) |\sin(\phi_j^{\mathcal{S}}) \sin(\phi_i^{\mathcal{Q}})|^2 , \end{aligned} \quad (\text{E2})$$

where we have denoted by $v_j^{\mathcal{S}} \bullet v_i^{\mathcal{Q}} \equiv \sum_{k=1}^{d^2-1} v_{j,k}^{\mathcal{S}} v_{i,k}^{\mathcal{Q}}$, with $\{v_{i,k}^{\mathcal{Q}}\}_{k=0}^{d^2-1}$ and $\{v_{j,k}^{\mathcal{S}}\}_{k=0}^{d^2-1} \in \mathbb{C}^{d^2-1}$. By denoting $c_{ij} \equiv \cos(\phi_j^{\mathcal{S}}) \cos(\phi_i^{\mathcal{Q}})$, $s_{ij} \equiv \sin(\phi_j^{\mathcal{S}}) \sin(\phi_i^{\mathcal{Q}})$, and $v_{ij} \equiv v_j^{\mathcal{S}} \bullet v_i^{\mathcal{Q}}$, we can use the (forward and reversed) triangle inequality, as follows

$$|c_{ij}| - |v_{ij} s_{ij}| \leq |c_{ij} + v_{ij} s_{ij}| \leq |c_{ij}| + |v_{ij} s_{ij}| . \quad (\text{E3})$$

By recalling that $c_{ij}, s_{ij} \geq 0$, since $\phi_i^{\mathcal{Q}}, \phi_j^{\mathcal{S}} \in [0, \pi/2]$, the second inequality yields $|c_{ij} + v_{ij} s_{ij}| \leq |c_{ij}| + |v_{ij} s_{ij}| = c_{ij} + |v_{ij}| s_{ij}$. If we assume that $|v_{ij}| \leq 1$, then the inequality becomes $|c_{ij} + v_{ij} s_{ij}| \leq c_{ij} + s_{ij}$. By squaring both sides, we get

$$|c_{ij} + v_{ij} s_{ij}|^2 \leq c_{ij}^2 + s_{ij}^2 + 2c_{ij} s_{ij} , \quad (\text{E4})$$

where this inequality is saturated iff $v_{ij} = 1$ for all $i = 1, \dots, K(\mathcal{Q})$ and $j = 1, \dots, K(\mathcal{S})$. Substituting back into Eq. (E2) and using the definitions of $\chi_{00}^{\mathcal{Q}}$ and $\chi_{00}^{\mathcal{S}}$ from Eq. (A11), as well as the fact that $\sum_i q_i^2 = \sum_j s_j^2 =$

d for CPTP maps \mathcal{Q} and \mathcal{S} , we arrive at

$$\chi_{00}^{\mathcal{S} \circ \mathcal{Q}} = \frac{1}{d} \sum_{i,j} s_j^2 q_i^2 |c_{ij} + v_{ij} s_{ij}|^2 \quad (\text{E5})$$

$$\leq \frac{1}{d} \sum_{i,j} s_j^2 q_i^2 (c_{ij}^2 + s_{ij}^2 + 2c_{ij} s_{ij}) \quad (\text{E6})$$

$$= \frac{1}{d} [\chi_{00}^{\mathcal{S}} \chi_{00}^{\mathcal{Q}} + (d - \chi_{00}^{\mathcal{S}})(d - \chi_{00}^{\mathcal{Q}})] + \frac{2}{d} \sum_{i,j} s_j^2 q_i^2 c_{ij} s_{ij} \quad (\text{E7})$$

$$= \frac{1}{d} [\chi_{00}^{\mathcal{S}} \chi_{00}^{\mathcal{Q}} + (d - \chi_{00}^{\mathcal{S}})(d - \chi_{00}^{\mathcal{Q}})] + \frac{2}{d} \left(\sum_j s_j^2 \cos(\phi_j^{\mathcal{S}}) \sin(\phi_j^{\mathcal{S}}) \right) \times \times \left(\sum_i q_i^2 \cos(\phi_i^{\mathcal{Q}}) \sin(\phi_i^{\mathcal{Q}}) \right) . \quad (\text{E8})$$

Next, we use the Cauchy-Schwartz inequality

$$\sum_i q_i^2 \cos(\phi_i^{\mathcal{Q}}) \sin(\phi_i^{\mathcal{Q}}) \quad (\text{E9})$$

$$= \sum_i (q_i \cos(\phi_i^{\mathcal{Q}})) (q_i \sin(\phi_i^{\mathcal{Q}})) \quad (\text{E10})$$

$$\leq \sqrt{\sum_i q_i^2 \cos^2(\phi_i^{\mathcal{Q}})} \sqrt{\sum_i q_i^2 \sin^2(\phi_i^{\mathcal{Q}})} \quad (\text{E11})$$

$$= \sqrt{\chi_{00}^{\mathcal{Q}} (d - \chi_{00}^{\mathcal{Q}})} , \quad (\text{E12})$$

where the Cauchy-Schwartz inequality is saturated when the vectors $\{q_i \cos(\phi_i^{\mathcal{Q}})\}_{i=1}^{K(\mathcal{Q})}$ and $\{q_i \sin(\phi_i^{\mathcal{Q}})\}_{i=1}^{K(\mathcal{Q})}$ are linearly dependent, therefore $\tan(\phi_1^{\mathcal{Q}}) = \dots =$

$\tan(\phi_{K(\mathcal{Q})}^{\mathcal{Q}})$. Since $\phi_i^{\mathcal{Q}} \in [0, \pi/2]$ for $\forall i = 1, \dots, K(\mathcal{Q})$ and the function $\tan(x)$ is one-to-one in that region, it follows that the above inequality is saturated iff $\phi_1^{\mathcal{Q}} = \dots = \phi_{K(\mathcal{Q})}^{\mathcal{Q}}$. The exact same argument for the channel \mathcal{S} yields

$$\sum_j s_j^2 \cos(\phi_j^{\mathcal{S}}) \sin(\phi_j^{\mathcal{S}}) \leq \sqrt{\chi_{00}^{\mathcal{S}} (d - \chi_{00}^{\mathcal{S}})} , \quad (\text{E13})$$

where the inequality is saturated iff $\phi_1^{\mathcal{S}} = \dots = \phi_{K(\mathcal{S})}^{\mathcal{S}}$. Substituting Eqs. (E12) and (E13) into Eq. (E8), we arrive at

$$d \chi_{00}^{\mathcal{S} \circ \mathcal{Q}} \leq \chi_{00}^{\mathcal{S}} \chi_{00}^{\mathcal{Q}} + (d - \chi_{00}^{\mathcal{S}})(d - \chi_{00}^{\mathcal{Q}}) + 2 \sqrt{\chi_{00}^{\mathcal{S}} \chi_{00}^{\mathcal{Q}} (d - \chi_{00}^{\mathcal{S}})(d - \chi_{00}^{\mathcal{Q}})} , \quad (\text{E14})$$

or equivalently,

$$\sqrt{d \chi_{00}^{\mathcal{S} \circ \mathcal{Q}}} \leq \sqrt{\chi_{00}^{\mathcal{S}}} \sqrt{\chi_{00}^{\mathcal{Q}}} + \sqrt{d - \chi_{00}^{\mathcal{S}}} \sqrt{d - \chi_{00}^{\mathcal{Q}}} . \quad (\text{E15})$$

Dividing both sides by d and redefining $\chi_{00}^{\mathcal{Q}}/d \equiv \cos^2(\delta^{\mathcal{Q}})$ for $\delta^{\mathcal{Q}} \in [0, \pi/2]$, as suggested in Eq. (13), we arrive at

$$\cos(\delta^{\mathcal{S} \circ \mathcal{Q}}) \leq \cos(\delta^{\mathcal{S}}) \cos(\delta^{\mathcal{Q}}) + \sin(\delta^{\mathcal{S}}) \sin(\delta^{\mathcal{Q}}) . \quad (\text{E16})$$

Using a triangle identity to simplify the right hand side, we get $\cos(\delta^{\mathcal{S} \circ \mathcal{Q}}) \leq \cos(\delta^{\mathcal{S}} - \delta^{\mathcal{Q}})$, i.e.

$$\delta^{\mathcal{S} \circ \mathcal{Q}} \geq |\delta^{\mathcal{S}} - \delta^{\mathcal{Q}}| , \quad (\text{E17})$$

which allows $\delta^{\mathcal{S} \circ \mathcal{Q}} \in [0, \pi/2]$ given $\delta^{\mathcal{S}}, \delta^{\mathcal{Q}} \in [0, \pi/2]$. In other words, given $\chi_{00}^{\mathcal{Q}}$ and $\chi_{00}^{\mathcal{S}}$, the composite channel χ -matrix element $\chi_{00}^{\mathcal{S} \circ \mathcal{Q}}$ is bounded from above by

$$\frac{\chi_{00}^{\mathcal{S} \circ \mathcal{Q}}}{d} \leq \cos^2 \left(\arccos \sqrt{\frac{\chi_{00}^{\mathcal{S}}}{d}} - \arccos \sqrt{\frac{\chi_{00}^{\mathcal{Q}}}{d}} \right) . \quad (\text{E18})$$